Phylogenomic analyses of the East Asian endemic *Abelia* (Caprifoliaceae) shed insights into the temporal and spatial diversification history with widespread hybridizations

Qing-Hui Sun[1], Diego F. Morales-Briones[2,3], Hong-Xin Wang[1,4], Jacob B. Landis[5,6], Jun Wen[7], Hua-Feng Wang[1]*

[1] *Key Laboratory of Tropical Biological Resources of Ministry of Education, College of Tropical Crops, Hainan University, Haikou 570228, China*

[2] *Department of Plant and Microbial Biology, College of Biological Sciences, University of Minnesota, 140 Gortner Laboratory, 1479 Gortner Avenue, Saint Paul, MN 55108, USA*

[3] *Systematics, Biodiversity and Evolution of Plants, Department of Biology I, Ludwig-Maximilians-Universität München, Menzinger Str. 67, 80638, Munich, Germany*

[4] *Zhai Mingguo Academician Work Station, Sanya University, Sanya 572022, China*

[5] *School of Integrative Plant Science, Section of Plant Biology and the L.H. Bailey Hortorium, Cornell University, Ithaca, NY 14850, USA*

[6] *BTI Computational Biology Center, Boyce Thompson Institute, Ithaca, NY 14853, USA*

[7] *Department of Botany, National Museum of Natural History, MRC-166, Smithsonian Institution, PO Box 37012, Washington, DC 20013-7012, USA*

*Authors for correspondence:

Hua-Feng Wang, E-mail: hfwang@hainanu.edu.cn

Abstract:

• **Background and Aims** *Abelia* (Caprifoliaceae) is a small genus with five species, including one man-made hybrid and several natural hybrids. The genus has a discontinuous distribution in mainland China, Taiwan Island, and the Ryukyu islands, providing a model system to explore mechanisms of species dispersal in the East Asian flora. However, the current phylogenetic relationships within *Abelia* remain uncertain.

• **Methods** In this study, we reconstructed phylogenetic relationships within *Abelia* using nuclear loci generated by target enrichment and plastomes from genome skimming. Divergence time estimation, ancestral area reconstruction, and ecological niche modelling (ENM) were used to examine the diversification history of *Abelia*.

• **Key Results** We found extensive cytonuclear discordance across the genus. By integrating lines of evidence from molecular phylogenies, divergence times, and morphology, we propose to merge *A. macrotera* var. *zabelioides* into *A. uniflora*. Network analyses suggested that there have been widespread and multiple hybridization events among *Abelia* species. These hybridization events may have contributed to the speciation mechanism and resulted in a high observed morphological diversity. The diversification of *Abelia* began in the early Eocene, followed by *A. chinensis* var. *ionandra* colonizing the island of Taiwan in the Middle Miocene. The ENM results suggested an expansion of climatically suitable areas during the Last Glacial Maximum and range contraction during the Last Interglacial. Disjunction between the Himalayan-Hengduan Mountain region (HHM) and the island of Taiwan is most likely the consequence of topographic isolation and postglacial contraction.

• **Conclusions** We used genomic data to reconstruct the phylogeny of *Abelia* and found a clear pattern of reticulate evolution in the group. In addition, our results support shrinkage of postglacial range and the heterogeneity of the terrain have led to the disjunction of the mainland China-Taiwan island. This study provides important new insights into the speciation process and taxonomy of *Abelia*.

Key words: *Abelia*; Gene tree discordance; Hybridization; Mainland China-Taiwan island disjunction.

INTRODUCTION

The underlying causes of disjunct distributions in various organisms have been a central issue in biogeography (e.g., Xiang et al., 1998; Wen, 2001; Qian and Ricklefs, 2004; Wang et al., 2012; Wen et al., 2013, 2018). Much discussion has focused on two mechanisms, vicariance and long-distance dispersal (Givnish and Renner, 2004; Yoder and Nowak, 2006; Šarhanová et al., 2017; Wang et al., 2020b). The emergence of geographic barriers leads to vicariance, resulting in decreased gene flow; while long-distance dispersal in plants usually involves rare events driven by dispersal vectors such as animals, wind or water currents (Nathan et al., 2008). Recent molecular systematic studies have shown that many plant disjunctions are too young to be explained by continental drift or major geographic barriers (Mummenhoff et al., 2004; Yoder and Nowak, 2006; Linder et al., 2013; Jiang et al., 2019). Hence, long-distance dispersal has emerged as a major mechanism to explain many discontinuous distributions in historical biogeography (Wen et al., 2013; Ye et al., 2019; Wen and Wagner, 2020).

Biogeographic disjunctions between mainland China-Taiwan island have received considerable attention with the separation of the two regions by 130 km (Wu and Wang, 2001; Xiang and Soltis, 2001; Qiu et al., 2011; Chen et al., 2012; Ye et al., 2014, Jin et al., 2020). The island of Taiwan is the largest subtropical mountainous island in the monsoonal western Pacific region, located on the Tropic of Cancer, having originated in the late Miocene (ca. 9-5 million years ago; Sibuet and Hsu, 2004). Molecular phylogenetic analyses have shown that several plant lineages have disjunct distributions between mainland China and Taiwan Island (e.g., *Sassafras* J. Presl, Nie et al., 2007; *Pseudotsuga* Carrière, Wei et al., 2010; *Triplostegia* Wall. ex DC., Niu et al., 2018; *Prinsepia*., Jin et al., 2020). Geologically, the island of Taiwan and its adjacent continental margin of mainland China belong to the Eurasian plate; in the Late Cretaceous both were part of the continental block. The continental block has undergone many extensions and rifting events since the Paleocene (Wei, 2010; Suo et al., 2015). Two hypotheses have been proposed to explain the formation of current plant disjunctions in this region: long-distance dispersal and postglacial contraction (Chou et al., 2011; Wang et al., 2013; Ye et al., 2014; Niu et al., 2018). A phylogeographic study of *Cunninghamia* R.Br. ex A.Rich. (Taxodiaceae) revealed that populations of Taiwan derived from continental Asia and colonized the island via long-distance seed dispersal (Lu et al., 2001). Factors that have major impacts on population dynamics and genetic variation patterns in plants in this region include past geological and climatic changes, uplift of the Qinghai-Tibet Plateau, global optimum temperature since the Miocene and the Quaternary glacial-interglacial transition (Xu et al., 2015; Cao et al., 2016; Chen et al., 2020). Recent studies have suggested that although the ice sheet was not ubiquitous from the Qinling Mountains and Huai River (at ca. 34° N) to the tropical south (≤ 22° N) in China during the Last Glacial period, the temperature in most parts of mainland China was lower than today (Shi et al., 2006). Temperature changes influence species distributions, population sizes, and intraspecific genetic differentiation. The postglacial contraction hypothesis states that many species had a continuous distribution from mainland China to Taiwan prior to the Quaternary glacial period, sometimes with disjunction between the Himalayan-Hengduan Mountain region and the island of Taiwan occurring when samples migrated to higher altitudes as global temperatures increased.

Abelia R.Br. belongs to the subfamily Linnaeoideae Raf. within Caprifoliaceae *s.l.* (Dipsacales; Yang and Landrein, 2011; Caprifoliaceae; Wang et al., 2020a, 2021). The genus includes *A. chinensis* (four varieties), *A. forrestii* (two varieties), *A.* × *grandiflora*, *A. macrotera* (eight varieties), *A. schumannii* and *A. uniflora* (Landrein et al., 2017; 2020; Fig. 1). *Abelia* is a typical East Asian endemic genus with a disjunct distribution in southwestern China, extending to the eastern portion of the island of Taiwan and the Ryukyu islands in Japan. The genus includes an important ornamental species, *Abelia* × *grandiflora*, widely cultivated in yards, parks and roadsides of temperate cities (e.g., Beijing, London, Washington D.C., and Wuhan). However, the phylogenetic relationships within *Abelia* remain unresolved due to limited DNA markers and sampling, and hence the biogeographic history and process of speciation are still unclear. Kim (1998) used one nuclear (ITS) and one plastid (*matK*) marker to infer the phylogenetic relationships within *Abelia*. However, species relationships could not be clarified because only two *Abelia* species were included, and a polytomy existed between the two *Abelia* species and those of *Diabelia*. Three *Abelia* species were included (*A. chinensis, A. engleriana* and *A. schumannii*) in Jacobs et al. (2010), but no information about relationships can be inferred since the three formed a polytomy. Using ITS and nine plastid regions, Wang et al. (2015) found that *A. forrestii* was sister to all other *Abelia* species, while *A. chinensis* was sister to *A.* × *grandiflora* with moderate support. Although Landrein (2017) included 46 samples (representing five species) of *Abelia* (22 from natural samples and 24 of horticultural breeds), using AFLP, ITS and three plastid genes, the species phylogeny was still unclear due to lack of resolution and low bootstrap support for many nodes.

Here, we explore the phylogenetic relationships and biogeographic diversification of *Abelia* using a target enrichment data set for nuclear loci and plastomes from genome skimming. We aim to (1) clarify the species-level phylogeny of *Abelia* based on nuclear genes and plastome data; and (2) reconstruct the biogeographic history of *Abelia* and explore the evolution of its distribution patterns related to the disjunction between mainland China and the island of Taiwan.

MATERIALS AND METHODS

Sampling, genomic data generation

We sampled 38 individuals from four species and one hybrid of *Abelia* (Landrein, 2017; 2020). Six Linnaeoideae species [*Diabelia serrata* (Siebold & Zucc.) Landrein, *D. sanguinea* (Makino) Landrein, *Kolkwitzia amabilis* Graebn., *Dipelta floribunda* Maxim. (two individuals), *Linnaea borealis* L., and *Vesalea occidentails* Villarreal] were used as outgroups. Vouchers of newly collected samples were deposited in the herbarium of the Institute of Tropical Agriculture and Forestry (HUTB), Hainan University, Haikou, China and Kew (K). Complete voucher information is listed in Supporting Information Table S1.

DNA was extracted from dried leaf tissue using a modified cetyltrimethylammonium bromide (CTAB) method, with chloroform: isoamyl alcohol separation and isopropanol precipitation at -20□ (Doyle and Doyle, 1987). We checked the concentration of each extraction with a Qubit 2.0 Fluorometer (Thermo Fisher Scientific, Waltham, MA, USA) and sonicated 400□ng of DNA using a Covaris S2 (Covaris, Woburn, MA) to produce fragments ~150 - 350□bp in length for making sequencing libraries. To ensure that genomic DNA was sheared to the appropriate fragment size, we evaluated all samples on a 1.2% (w/v) agarose gel.

We used a Hyb-Seq approach (Weitemier et al., 2014) combining target enrichment and genome skimming, which allows simultaneous data collection for low-copy nuclear genes and high-copy genomic targets. To obtain nuclear data from target enrichment, we ran MarkerMiner v.1.2 (Chamala et al., 2015) with default settings to identify putative single copy nuclear (SCN) genes using the transcriptome of *Lonicera japonica* from 1KP (He et al., 2017), and the genome of *Arabidopsis thaliana* (L.) Heynh. (Gan et al., 2011). We then used GoldFinder (Vargas et al., 2019) to further filter the SCN genes identified by MarkerMiner. Finally, we obtained 428 putatively single-copy orthologous genes in total for phylogenetic analysis (Wang et al., 2021). Hybridization, enrichment, and sequencing methods followed those of Wang et al. (2021). We obtained full plastomes from genome skimming data (Wang et al., 2021) with detailed descriptions of plastome sequencing methods in Wang et al. (2020a, 2020b).

Read processing and assembly

Raw sequencing reads were cleaned using Trimmomatic v.0.36 (Bolger et al., 2014) by removing adaptor sequences and low-quality bases (ILLUMINACLIP: TruSeq_ADAPTER: 2:30:10 SLIDINGWINDOW: 4:5 LEADING: 5 TRAILING: 5 MINLEN: 25). Nuclear loci were assembled with HybPiper v.1.3.1 (Johnson et al., 2016). Individual exon assemblies were used to avoid chimeric sequences in multi-exon genes produced by potential paralogy (Morales-Briones et al., 2018) and only exons with a reference length of more than 150 bp were assembled. Paralog detection was performed for all exons with the ‘paralog_ investigator’ warning. To obtain ‘monophyletic outgroup’(MO) orthologs (Yang and Smith, 2014), all assembled loci (with and without paralogs detected) were processed following Morales-Briones et al. (2021).

For plastome assembly, raw reads were trimmed using SOAPfilter_v2.2 (BGI, Shenzhen, China). Adapter sequences and low-quality reads with Q-value ≤ 20 were removed. Clean reads were assembled against the plastome of *Kolkwitzia amabilis* (KT966716.1) using MITObim v.1.8 (Hahn et al., 2013). Assembled plastomes were preliminarily annotated with Geneious R11.04 (Biomatters Ltd., Auckland, New Zealand) to detect possible inversions/rearrangements, with corrections of start/stop codons based on published *Abelia* plastomes (*A. chinensis*, accession No. MN384463.1; *A. forrestii*, accession No. MN524636.1; *A.* × *grandiflora*, accession No. MN524635.1; *A. macrotera*, accession No. MN524637.1).

Phylogenetic analyses

Nuclear data set. We analyzed the nuclear data set using concatenation and coalescent-based methods. Individual exons were aligned with MAFFT v.7.037b (Katoh and Standley, 2013) and aligned columns with more than 90% missing data were removed using Phyutility (Smith and Dunn, 2008) prior to concatenation. Maximum likelihood (ML) analysis was conducted using IQ-TREE v.1.6.1 (Nguyen et al., 2015) while searching for the best partition scheme (Lanfear et al., 2012) followed by ML gene tree inference and 1000 ultrafast bootstrap replicates (Hoang and Chernomor 2018). Additionally, we used Quartet Sampling (QS; Pease et al., 2018) to distinguish strong conflict from weakly supported branches. We carried out QS with 1000 replicates. We used ASTRAL-III v.5.7.1 (Zhang et al., 2018) for species tree estimation, with the input being individual exon trees generated with RAxML using a GTRGAMMA model.

Plastome data set. Contiguous contigs were aligned with MAFFT v.7.407 (Katoh and Standley, 2013) and columns with more than 90% missing data were removed using Phyutility. We performed extended model selection (Kalyaanamoorthy et al., 2017) followed by ML gene tree inference and 200 non-parametric bootstrap replicates for branch support in IQ-TREE. Additionally, we evaluated branch support with QS using 1,000 replicates.

Species network analysis

Due to computational restrictions and given our primary focus on potential reticulation between species, we reduced the 45 taxa data set to one outgroup and 14 ingroup samples representing all major clades based on the nuclear analyses. We looked for evidence of hybridization within *Abelia* via species network searches carried out with the InferNetwork_MPL function in PhyloNet (Wen et al., 2018). Network searches were carried out using only nodes in the gene trees that had at least 50 percent bootstrap support, enabling up to five hybridization events and optimizing the branch lengths and probabilities of inheritance of the returned species networks under the full probability. To disentangle nested hybridization, we also created a reduced, 12 sample data set by removing three known hybrids (*A.*× *grandiflora* E159, *A.*× *grandiflora* E227 and *A. chinensis* E206; see results) and carried out analyses as previously described. We used the command 'CalGTProb' in PhyloNet to calculate the probability scores of the concatenated tree, ASTRAL, and plastid trees to estimate the optimal number of hybridization events and to test if the network model explained our gene trees better than a purely bifurcating tree. We selected the best-fit-species network model using the lowest values for bias-corrected Akaike information criterion (AICc; Sugiura, 1978), Akaike information criterion (AIC; Akaike, 1998), and the Bayesian information criterion (BIC; Schwarz, 1978).

Divergence time estimation

To examine the historical biogeography of *Abelia*, we performed a dated phylogenetic analysis using BEAST v.1.8 (Drummond et al., 2012). As there is potential ancient hybridization in *Abelia*, we estimated dates separately using the nuclear and plastid data. We selected the fruit fossil of *Diplodipelta* from the late Eocene Florissant flora of Colorado (Manchester, 2000; Bell and Donoghue, 2005) to calibrate the node containing *Diabelia* and *Dipelta*, as the fossil shows morphological similarities to those two genera. We set a lognormal prior for the divergence at the stem of *Diabelia* and its sister clade *Dipelta* (offset

36 Ma, log-normal prior distribution 34.07-37.20 Ma). The ancestral node of Linnaeoideae (the root of our tree) was constrained to 50.18 Ma (mean 50.18 Ma) from results of previous studies (Wang et al., 2021) despite the lack of fossil evidence. The BEAST analyses were performed using an uncorrelated log normal (UCLN) relaxed clock with a Yule tree prior, a random starting tree, and GTR + G as model of sequence evolution (as selected by MrModelTest v.2.3; Nylander et al., 2004). Each MCMC run was conducted for 100,000,000 generations with sampling every 5,000 generation. The first 10% of trees were discarded as burn-in. We used Tracer v.1.6 to assess convergence and effective sample size (ESS) > 200 (Rambaut et al., 2014). Tree Annotator v.1.8.0 (Drummond et al., 2012) was used to summarize the set of post-burn-in trees and their parameters to produce a maximum clade credibility chronogram showing the mean divergence time estimates with 95% highest posterior density (HPD) intervals.

Ancestral area reconstructions

We reconstructed the historical biogeography of *Abelia* using Bayesian binary MCMC (BBM) analysis implemented in RASP v.3.21 (Yu et al., 2015). To account for phylogenetic uncertainty, 5,000 out of 20,000 post-burn-in trees from the BEAST analyses (nuclear data) were randomly chosen for the BBM analyses. We compiled distribution data for the species of *Abelia* and assigned the included taxa to their respective ranges. Considering the areas of endemism in *Abelia* and tectonic history of the continent, we used three areas: (A) southwestern China, (B) central-eastern China, and (C) Taiwan and Ryukyu islands. Each sample was assigned to its respective area according to its contemporary distribution range (Table 1). We set the root distribution to null, applied 10 MCMC chains each run for 100 million generations, sampling every 10,000 generations using the JC + G model. The MCMC samples were examined in Tracer v.1.6 (Drummond et al., 2012) to confirm sampling adequacy and convergence of the chains to a stationary distribution.

Ecological niche modelling

We performed Ecological Niche Modelling (ENM) on *Abelia* using MAXENT v.3.2.1 (Phillips et al., 2006). For the input we obtained 200 species occurrence data points from the Chinese Virtual Herbarium (CVH, https://www.cvh.ac.cn/), Global Biodiversity Information Facility (http://www.gbif.org/) and field observations. The details of these occurrence data are listed in Table S1. We used 19 bioclimatic variables as environmental data for ENM representing five different time periods. Past and current data for these variables were available from the WorldClim database (http://worldclim.org/). The data included baseline climate (BioClim layers for the period 1950-2000 at a spatial resolution of 30 s arc), data for the last glacial maximum (LGM; ~22 000 years BP) with spatial resolution at 2.5 min arc resolution simulated by Community Climate System Model (CCSM), Max Planck Institute Model (MPI) and Model for Interdisciplinary Research on Climate (MIROC), and the last interglacial period. Replicate runs (25) of MAXENT were performed to ensure reliable results. Model performance was assessed using the area under the curve (AUC) of the receiver operating characteristic. AUC scores may range between 0.5 (randomness) and 1 (exact match), with those above 0.9 indicating good performance of the model (Swets, 1988). The MAXENT jackknife analysis was used to evaluate the relative importance of the 19 bioclimatic variables employed. All ENM predictions were visualized in ArcGIS v.10.2 (ESRI, Redlands, CA, USA).

Data accessibility

Raw Illumina data from target enrichment is available at the Sequence Read Archive (SRA) under accession PRJNA706913 (see Table 1 for individual sample SRA accession numbers). DNA alignments, phylogenetic trees and results from all analyses and datasets can be found in the Dryad data repository.

RESULTS

Exon assembly

The number of assembled exons per sample ranged from 253 (*A. macrotera* var. *macrotera* E45) to 992 (*A. uniflora* E46) (with > 75% of the target length), with an average of 851 exons per sample (Table S2; Fig. S1). The number of exons with paralog warnings ranged from six in *A. macrotera* var. *macrotera* E45 to 698 in *A. uniflora* E46 (Table S2). The concatenated alignment had a length of 365,330 bp, including 22,045 parsimony-informative sites, and a matrix occupancy of 83% (Table 2). The smallest locus had a length of 150 bp, while the largest locus had a length of 3,998 bp. The plastid alignment resulted in a matrix of 163,130 bp with 3,850 parsimony-informative sites and a matrix occupancy of 96% (Table 2).

Phylogenetic reconstruction

We inferred the phylogeny of *Abelia* based on nuclear and plastid alignments (Figs. 2-3 and S2-S3). Despite the generally well-supported topology, the positions of clades representing *A.* × *grandiflora*, *A. uniflora* and *A. macrotera* are unstable across the different phylogenetic analyses. Phylogenetic reconstruction based on the concatenated nuclear data showed all of the major clades are strongly supported (BS ≥ 75%; Fig. 2, Left). *Abelia chinensis* forms a clade with *A.* × *grandiflora*; and *A. macrotera* var. *zabelioides* is sister to *A. uniflora* with the clade having strong QS support but also a signal of a possible alternative topology (0.97/0/1, Fig. S2, Left). The *A. chinensis* + *A.* × *grandiflora* clade is then sister to the *A. macrotera* var. *zabelioides* + *A. uniflora* clade (Fig. 2, Left).

The ASTRAL analyses (Fig. 3) recovered all major clades with strong support (local posterior probabilities, LPP ≥ 0.95). *Abelia forrestii* is sister to the *A. macrotera* clade, which is then sister to the *A. macrotera* var. *zabelioides* + *A. uniflora* clade. The *A. chinensis* + *A.* × *grandiflora* clade is sister to the clade of all remaining species. The clade composed of *A. chinensis* + *A.* × *grandiflora* has moderate QS support for a signal of a possible alternative topology (0.33/0.06/0.99). The clade composed of *A. macrotera* var. *zabelioides* + *A. uniflora* has strong QS support but a signal of a possible alternative topology (0.98/0/1). The sister relationship of the *A. macrotera* var. *zabelioides* + *A. uniflora* has QS counter support as a clear signal for alternative topology (-0.21/0.32/0.99).

For the plastid tree (Fig. 2, Right and S3), *A. macrotera* var. *zabelioides* is nested within *A. uniflora*, with the clade having strong QS support signaling an alternative topology (0.51/0.35/0.98). The *A. chinensis* + *A.* × *grandiflora* clade shows a sister relationship with the *A. macrotera* var. *zabelioides* + *A. uniflora* + *A. macrotera* clade, with strong QS support (0.75/0.51/0.98). The results strongly support *A. forrestii* from Yunnan, China as sister to the remainder of the genus with the QS analysis providing full support (1/–/1, Fig. S3).

In our species network analyses (including both 15 and 12 samples), all networks with one to five reticulation events were shown to be a better model than a strictly bifurcating tree (Table 3; Figs. 4 and S4-S5). Four reticulation events were inferred for the best network in the 15 samples tree, two reticulation-events involving *A.* × *grandiflora*, the third reticulation event occurred to *A. chinensis* and the fourth revealed ancestral gene flow to the *A.* × *grandiflora* clade (Fig. 4A). For *A.* × *grandiflora* E159, the inheritance probability analysis showed that the major genetic contributor (57.2%) came from the ancestor of *A.* × *grandiflora* and a minor contribution was from the *A. macrotera* clade (42.8%). For *A.* × *grandiflora* E227, the major genetic contributor came from *A. uniflora* (53.6%). For *A. chinensis* E206, the major genetic contributor (53.0%) came from the ancestor of *A.* × *grandiflora*. For the ancestor of the *A.* × *grandiflora* clade, the major genetic contributor was a putative ancestor of *A. chinensis* (74.1%) with a minor contribution from *A. uniflora* (25.9%). In the 12 samples tree (Fig. 4B), we removed the known hybrids from the previous analyses by excluding *A.* × *grandiflora* E159, *A.*× *grandiflora* E227 and *A. chinensis* E206, and then discovered that the best network had three reticulation events. There appears to be abundant gene flow in the backbone of *Abelia* and the 12 samples analyses showed that *A. macrotera*, *A. uniflora* and *A. chinensis* were each derived from complex hybridization events.

Divergence time estimation

Divergence times were estimated using BEAST v.1.8 which takes into account phylogenetic and calibration uncertainties. Given that *A.* × *grandiflora* is an artificial hybrid, the taxon should not be included in the divergence time estimation and ancestral area reconstruction analysis of the genus.

Divergence time estimates based on the nuclear tree (Fig. 5) suggested that the ancestor of *Abelia* originated 33.47 Ma (95% HPD: 23.53-38.21 Ma, node 1). The divergence of *A. chinensis* clade from the remaining *Abelia* species could be dated to 29.56 Ma (95% HPD: 21.64-33.76 Ma, node 2). *Abelia forrestii* diverged from its close relatives 24.93 Ma (95% HPD: 18.62-29.16; node 3). The split between *A. uniflora* and *A. macrotera* var. *zabelioides* was 14.93 Ma (95% HPD: 12.39-20.21 Ma, node 6). *Abelia macrotera* diverged from its close relatives 23.51 Ma (95% HPD: 16.91-27.09; node 4). *Abelia chinensis* var. *ionandra* diverged from its close relatives 12.44 Ma (95% HPD: 8.61-17.03 Ma, node 7). A comparison of the divergence time estimates using the chloroplast tree is shown in Fig. S6. For instance, the age of the stem group of *Abelia* was dated to 45.10 Ma (95% HPD: 34.91-50.09 Ma, node 1). *Abelia forrestii* diverged from its close relatives 29.75 Ma (95% HPD: 21.64-39.04; node 2). The split between *A. uniflora* and *A. macrotera* var. *zabelioides* was 14.31 Ma (95% HPD: 8.16-23.08 Ma, node 6).

Ancestral area reconstruction

According to our ancestral area reconstructions paired with divergence time estimation, *Abelia* originated around the early Eocene (Fig. 5) in mainland China (Fig. 6). Our analyses revealed two dispersal events and three vicariance events among the three defined biogeographic areas (Fig. 6). The ancestor of *Abelia* was inferred to have been present throughout region A (Yunnan, Chongqing, Sichuan, Guizhou and Hubei) and B (Jiangxi and Fujian), with subsequent dispersal or vicariance across southeastern China. The results indicate a southwestern and central-eastern China origin for the genus *Abelia*.

Ecological niche modelling and niche identity tests

The AUC test result (mean ± SD) for the ENM, averaged across all 25 runs, was significant (0.996 ±0.000 for *A. chinensis* and 0.993± 0.001 for *A. uniflora*) (Figs. 7 and S7), which supports the predictive power of the model. The MaxEnt analyses show that the current distribution prediction is largely identical to the recorded distribution of *Abelia*, and expansion beyond the existing range is also reasonable, including *A. uniflora* populations along the narrow coastline of eastern China and Japan (Fig. S7). In our analysis, the LGM climate and the present time climate species distribution areas show different distribution patterns. We used CCSM, MIROC and MPI models to simulate the LGM climate for the five species of *Abelia*, and the inferred distribution from the two LGM models (CCSM and MPI models) were highly similar. For the CCSM and MIROC models (the MIROC model area simulation during the LGM period is warmer and drier than the CCSM model), the distribution density and range of *Abelia* under the MPI model was slightly lower than the those generated from the CCSM model, but the differences were not significant (Fig. S7). Compared with the LGM climate, the potential distribution range of *Abelia* species in mainland China will be much smaller, while the habitat remains stable in most of the present time climate distributions.

DISCUSSION

Phylogenetic relationships within Abelia

Abelia is a genus in the Sino-Japanese Floristic Region with a disjunct distribution between the Himalaya-Hengduan Mountains and Taiwan (Kim et al., 1998; Wang et al., 2015). The genus was established by R. Brown in 1818 with *A. chinensis* R. Brown as the type species. Based on morphological features, *Abelia* was considered to be closely related to *Linnaea* (Rehder, 1911). Hu (1988) divided *Abelia* into two genera: *Abelia* s.s. and *Zabelia* (Rehd.) Makino. Later, Kim (1998) found that *Abelia* was sister to *Diabelia* based on a number of traditionally used morphological characters (mostly inflorescence traits) and molecular data. Previous studies did not resolve relationships within *Abelia*, likely because of the limited informative sites in the loci used (Kim, 1998; Jacobs et al., 2010; Wang et al., 2015; Landrein, 2017).

This study resolved well-supported phylogenetic relationships within *Abelia* using both nuclear and plastid data (Figs. 2-3 and S2-S3). The inferred topologies of the four recognized species in the nuclear and plastid trees are not entirely congruent (Figs. 2-3 and S2-S3). For instance, in the nuclear concatented tree (Fig. 2, Left), *Abelia macrotera* var. *zabelioides* is sister toand the *A. uniflora* form a clade, with the nodes having strong QS support values (Fig. 3). In the plastid tree (Figs. 2, Right) and the ASTRAL tree (Fig. 3), *Abelia macrotera* var. *zabelioides* is nested within *A. uniflora*. Cytonuclear discordance has been widely detected in plants (Lee et al., 2019; García et al., 2017; Hodel et al., 2021; Wang et al., 2021). The three main reasons for cytonuclear discordance are gene duplication/extinction, horizontal gene transfer/hybridization, and incomplete lineage sorting (ILS), but sources of such discordance remain hard to disentangle, especially when multiple processes co-occur (Degnan and Rosenberg, 2009).

Abelia macrotera var. *zabelioides* and *A. uniflora* share a recent common ancestor (Landrein et al., 2017), which is consistent with the results of our phylogenetic analysis (Figs. 2-3 and S2-S3). The species network analysis (Fig. 4) showed the two species are formed by different hybridization events.

Hybridization and introgression

There are controversial taxa or species complexes in *Abelia*. The *A. uniflora* complex is the most enigmatic in the genus, though it was only briefly described by Wallich (1829). Members of the *A. uniflora* complex are often difficult to identify with morphological characters alone. The morphological differences among entities within the *A. uniflora* complex can be explained by one or several historical or ongoing evolutionary processes. Specifically, the null taxonomic hypothesis is that the *A. uniflora* complex is a single hyperdiverse species (Link-Pérez, 2010), while the alternative is that speciation has occurred or is underway. We expect to detect clear genetic differentiation, which may be stronger if speciation is complete, or weaker when speciation is ongoing or confounded by introgression (Nosil, 2008; Liu et al., 2018). Based on morphological evidence and AFLP data, Landrein et al. (2017) indicated that *A. uniflora* shows evidence of formation due to hybridization/ introgression between *A. macrotera* and *A. chinensis*. Additionally, Landrein et al. (2017) showed that *A. forrestii* occurs in the contact zone between *A. macrotera* and *A. chinensis*, leading to a potential hypothesis of hybrid/introgression origin for *A. forrestii* from *A. macrotera* and *A. chinensis*.

In our analysis, it was found that there may be widespread cytonuclear discordance exists across *Abelia* (Figs. 2-3 and S2-S3). The discordance of the phylogeny may be caused by ILS or hybridization. Hybridization, introgression, and horizontal gene transfer are all examples of gene flow across populations that may be modeled by phylogenetic networks. Sols-Lemus et al. (2017) proposed that a minor contribution (~ 0.10) from a parental population to a reticulate node may indicate an introgression event based on inheritance probabilities. Inheritance probabilities near 0.50 may indicate that the reticulate node is the result of hybrid speciation between the parental populations. Our results show that the parental contributions to the reticulation events detected in *Abelia* (Fig. 4A) are essentially equal. For *A.* × *grandiflora* E159, the inheritance contributions (0.428 and 0.572) support a hybridization event between the ancestral lineage of the *A. macrotera* clade and *A. chinensis* E206. For *A.* × *grandiflora* E227, the inheritance contributions (0.536 and 0.464) support a hybridization event between *A. uniflora* and the ancestral lineage of the *A. chinensis* clade. For *A. chinensis* E206, the inheritance contributions (0.572 and 0.470) support a hybridization event between *A.* × *grandiflora* E227 and *A. chinensis* E111. For the ancestor of the *A.* × *grandiflora* clade, the reticulation event reveals that there has been extensive gene flow between the *A. chinensis* clade and *A. uniflora*. However, *A. uniflora* has less genetic contribution (0.259), suggesting that ancestral gene flow from *A. uniflora* to the ancestor lineage of the *A.* × *grandiflora* clade could also produce the observed results (Fig. 4A).

Because inheritance probability can be influenced by many biological factors, additional biological information is needed to interpret these values reliably (Sols-Lemus et al., 2017). In the 12 samples tree (Fig. 4B), we discovered that the ancestral lineage of *A. macrotera*, *A. uniflora* and *A. chinensis* were each derived from complex hybrid origins, which can explain the complicated taxonomy of the group.

Diversification history of Abelia

In this study, the dating results are incongruent between the nuclear and plastid analyses, with the nodes in the plastid tree generally showing older dates than those in the nuclear tree. Generally, chloroplast genes have shortcomings such as low selection pressure, single-parent inheritance, and slow inheritance rate (Lanier and Knowles, 2012; Wang and Liu, 2016), therefore we chose nuclear data for our dating analysis. Our analyses indicate that the stem of *Abelia* dates to the early Eocene 33.47 Ma (95% HPD: 23.53-38.21 Ma) (Fig. 5). Most of the diversification events within *Abelia* were dated to the early to middle Miocene (Fig. 5).

Our phylogenetic analyses indicate that *A. chinensis* var. *ionadra* from the island of Taiwan is sister to *A. chinensis* from Jiangxi province, China (Figs. 2-3 and S2-S3). In addition, previous phylogenetic and phylogeographic studies have generally shown that existing populations of many species on the island of Taiwan are descendants of mainland China (e.g. in *Taiwania*, Chou et al., 2011; *Sassafras*, Nie et al., 2007; *Dichocarpum arisanense*, Xiang et al., 2017; *Triplostegia*, Niu et al., 2018), with few reports supporting a reverse scenario. Based on our divergence time estimates, the stem age of *A. chinensis* var. *ionadra* was dated to the middle Miocene, ca. 12.44 Ma (Fig. 5, node 7), which greatly predates the formation of the island of Taiwan, having originated in the late Miocene (Sibuet and Hsu, 2004). A similar pattern was shown in *Tinospora dentata* which split from its Japanese relatives in the early Miocene around 38.97 Ma (95% HPD: 26.45-52.52) (Wang et al., 2017).

The island of Taiwan is located at the eastern edge of the Eurasian plate and the Taiwan Strait could have first occurred in the late Mesozoic (Ye, 1982; Suo et al., 2015). Owing to the intense tectonic movements, contacts between the island of Taiwan and mainland China occurred during the late Cretaceous-Early Paleocene and late Eocene-early Oligocene (Teng, 1992). One hypothesis that has been put forward is that tropical rainforests in the Indo-Malayan region may have appeared near the Cretaceous-Paleogene (K-Pg) boundary (Wang et al., 2012). Plant macrofossils that are closely related to extant subtropical species have been recorded from Taiwan during the early Miocene, while pollen fossils date to the Oligocene (Li, 2000). Due to the landmass being subjected to stretching and rifting (Ye, 1982; Teng, 1992; Suo et al., 2015), part of the mountain ranges on the island of Taiwan represents a relict area of the ‘Taiwan-Sinzi Folded Zone’ (Ye, 1982; Teng, 1992; Li and Wen, 2016), which facilitated a cooler climate in Asia during the late Eocene (Zachos et al., 2001). Around this time, a vicariance event between Taiwan and mainland China may have occurred. Based on the results of our *Abelia* sequencing, the Taiwan (Yilan) flora may contain relatively ancient components (Li and Wen, 2016). The flora of mainland China has been acknowledged to have contributed to Taiwan’s floristic assembly (Li and Keng, 1950). The Luzon arc did not begin to collide with the Eurasian plate until the late Miocene (9-6 Ma) (Sibuet et al., 2002). Thus, we hypothesize that the relatively young gene flow in the flora of Taiwan may be derived from plants in mainland China. This hypothesis needs further validation by combining phylogenetic and molecular dating methods, as well as by studying other plant groups, particularly more ancient lineages.

The stem group of *Abelia* is dated to have formed during the early Eocene (33.47 Ma, 23.53-38.21 Ma; node 1), later than the early uplift of the Qinghai-Tibet Plateau (QTP). However, ancestral area reconstructions revealed that the *A. uniflora* complex might have colonized southwestern China, central-eastern China, and Taiwan and Ryukyu islands (Fig. 6).

Potential refugia and demographic history

Many botanists and biogeographers have explained the discontinuous distribution pattern of plants in East Asia and North America from different perspectives (Xiang et al., 1998; Wen, 2001; Nie et al., 2007; Sessa et al., 2012). It is hypothesized that East Asia was less affected by the Quaternary glaciations than North America and Nordic Europe, except in alpine areas (Shi et al., 2006).

Climate shifts in the Quaternary and associated environmental changes may have driven the diversification of *Abelia*. Diversification would have been sustained by Pleistocene glaciations because species habitats underwent expansion and contraction, leading to populations flourishing, migrating or extincting (Comes et al., 2008; Qiu et al., 2011).

Our ENM analysis provides a detailed hypothesis during the last glacial cycle (Figs. 7 and S7). The results suggest that extant populations likely differentiated well before the LGM and also provide strong evidence for survival of *Abelia* in southwest China during the LGM (Fig. S8). Therefore, the climatic shock during the LGM may have had a significant impact on the recent history of *Abelia* at the population level compared with an earlier period of species differentiation (Qiu et al., 2011). Potential habitat for *A. forrestii* spanned most of southwest China during the LGM period. However, its current distribution is only in Yunnan and Sichuan of southwestern China from 1900 to 3300 m in altitude. *Abelia chinensis* and *A. uniflora* were distributed in mainland China and Southern Japan during the LGM period (Fig. 7). However, the current distribution area has shrunk, which highlights the importance of topographic complexity in promoting species differentiation both by increasing habitat diversity and limiting gene flow between elevation-restricted populations (Ye et al., 2019). Yunnan, Guizhou, Sichuan and Guangxi are placed in the East Asiatic region in terms of phylogenetic regionalization, but are placed in the Paleotropic region for taxonomic regionalization. Because these areas possess more endemism, particularly paleoendemic genera (Ying et al., 1994), they are thought to have been a refuge during the Pleistocene glacial period (López-Pujol and Ren, 2010; Ye et al., 2019). For *A. macrotera*, there is few significant change when comparing its LGM distribution to that in the current period. Thus, we hypothesize that the refugia reflect the evolutionary history of *A. macrotera*. This hypothesis needs to be further tested by studying additional plant groups, especially ancient lineages, through the integration of plastome and adequate nuclear data to balance the preferences towards nuclear/chloroplast genomes. In addition, *Abelia chinensis* var. *ionandra* has expanded to the coastal regions of East China and reached Taiwan via land bridges across the Taiwan Strait during the glacial period. Due to repeated glacial-interglacial cycles, mainland China and Taiwan populations may have experienced frequent gene flow through a continental bridge during Quaternary. After the LGM, *Abelia* populations in southeastern China may have experienced a large-scale extinction event, and Jiangxi may be a glacial refuge for *A. chinensis*. The uplift of the QTP was a consequence of the collision of the Indian subcontinent with the Eurasian plate 40-50 million years ago (Yin and Harrison, 2000; Fu et al., 2020). Because of multiple asynchronous expansions, multiple independent refugia *in situ* and complex topography in this region might explain why accurate analyses of species distribution patterns are difficult (Cun and Wang, 2010; Yan et al., 2012). Because *Abelia* does not have a strong ability of pollen or seed transmission, the present distribution pattern of *A. chinensis* var. *ionandra* may be the result of topographic isolation and postglacial contraction.

CONCLUSIONS

Natural hybridization/infiltration is extensive in *Abelia* and may require further investigation with extensive populational sampling. Our findings support the use of Hyb-Seq data at the population level to clarify the boundaries among species complexes. For other taxa, our study demonstrates the importance to use both nuclear and plastid genome data, as well as network analysis, to untangle the potential reticulation history. Our results also indicate that several interglacial refuges in *Abelia* have been identified in the middle of the Hengduan Mountains. Besides, our research provide a theoretical foundation for investigating the disjunctively distributed plants between Taiwan island and mainland China, as well as supporting hypotheses of postglacial range contraction together with topographic heterogeneity being responsible for the observed disjunction.

TAXONOMIC TREATMENT

Abelia uniflora R. Br. in Wall., Pl. As. Rar. 1. 15. 1830. -Type: China, Fujian, [‘Ngan-Ke-Kyen’Black Tea Country], *Reeves s.n.* (holotype: CGE!, isotype: BM!).

=*Abelia macrotera* (Graebn. & Buchw.) Rehder var. *zabelioides* Landrein, Kew Bull. 74(4)-70: 93. 2019. Type: China, Sichuan, Leshan Pref., E’mei Shan, 21 June 1938, *H. C. Chow 7573* (holotype: A!). **Synonym nov.**

Author contributions

H.F.W. and J.W. conceived the study. H.F.W. and D.F.M-B. performed the research and analyzed the data. Q.H.S., D.F.M-B., H.X.W., J.W. J.B.L, and H.F.W. wrote and revised the manuscript.

ACKNOWLEDGEMENTS

The work was funded by National Science Foundation of China (31660055) and Hainan Provincial Natural Science Foundation of China (421RC486). We appreciate Gabriel Johnson for his help with the target enrichment experiment, and the United States National Herbarium for collection access. We acknowledge the staff in the Laboratories of Analytical Biology at the National Museum of Natural History, the Smithsonian Institution for technical support and assistance.

REFERENCES

Akaike H. 1998. Information theory and an extension of the maximum likelihood principle. *Selected papers of hirotugu akaike* 199-213.

Bell CD, Donoghue MJ. 2005. Phylogeny and biogeography of Valerianaceae (Dipsacales) with special reference to the South American valerians. *Organisms Diversity and Evolution* **5**: 147-159.

Cao YN, Wang IJ, Chen LY, Ding YQ, Liu LX, Qiu YX. 2016. Inferring spatial patterns and drivers of population divergence of *Neolitsea sericea* (Lauraceae), based on molecular phylogeography and landscape genomics. *Molecular Phylogenetics and Evolution* **126**: 162-172.

Chen XD, Yang J, Feng LI, Zhou T, Zhang H, Li HM, Bai GQ, Meng X, Li ZH, Zhao GF. 2020. Phylogeography and population dynamics of an endemic oak (Quercus fabri Hance) in subtropical China revealed by molecular data and ecological niche modeling. *Tree Genetics Genomes* **16**: 1-132.

Chen ZD, Ying JS, Lu AM. 2012. Disjunct distribution of seed plants between southwestern China and Taiwan Island island of China. *Chinese Journal of Botany* **47**: 551-570.

Chou YW, Thomas PI, Ge XJ, LePage BA, Wang CN. 2011. Refugia and phylogeography of Taiwania in East Asia. *Journal of Biogeography* **38**: 1992-2005.

Comes HP, Tribsch A, Bittkau C. 2008. Plant speciation in continental island floras as exemplified by *Nigella* in the Aegean Archipelago. *Philosophical Transactions of the Royal Society B: Biological Sciences* **363**: 3083-3096.

Cun YZ, Wang XQ. 2010. Plant recolonization in the Himalayan from the southeastern Qinghai-Tibetan Plateau: geographical isolation contributed to high population differentiation. *Molecular Phylogenetics and Evolution* **56**: 972-982.

Degnan JH, Rosenberg NA. 2009. Gene tree discordance, phylogenetic inference and the multispecies coalescent. *Trends in Ecology and Evolution* **24**: 332-340.

Doyle JJ, Doyle J. 1987. A rapid DNA isolation procedure for small quantities of fresh leaf tissue. *Phytochemical Bulletin* **19**: 11-15.

Drummond AJ, Suchard MA, Xie D, Rambaut A. 2012. Bayesian phylogenetics with BEAUti and the BEAST 1.7. *Molecular Biology Evolution* **29**: 1969-1973.

Fu PC, Sun SS, Khan G, Dong XX, Tan JZ, Favre A, Zhang FQ, Chen SL. 2020. Population subdivision and hybridization in a species complex of Gentiana in the Qinghai-Tibetan Plateau. *Annals of botany* **125**: 677-690.

Gan X, Stegle O, Behr J, Steffen JG, Drewe P, Hildebrand KL, Lyngsoe R, Schultheiss SJ, Osborne EJ, Sreedharan VT. 2011. Multiple reference genomes and transcriptomes for *Arabidopsis thaliana*. *Nature* **477**: 419-423.

García N, Folk RA, Meerow AW, Chamala S, Gitzendanner MS, de Oliveira RS, Soltis DE, Soltis PS. 2017. Deep reticulation and incomplete lineage sorting obscure the diploid phylogeny of rain-lilies and allies (Amaryllidaceae tribe Hippeastreae). *Molecular Phylogenetics and Evolution* **111**: 231-247.

Givnish TJ, Renner SS. 2004. Tropical intercontinental disjunctions: Gondwana breakup, immigration from the boreotropics, and transoceanic dispersal. *International Journal of Plant Sciences* **165**: S1-S6.

Hahn C, Bachmann L, Chevreux B. 2013. Reconstructing mitochondrial genomes directly from genomic next-generation sequencing reads: a baiting and iterative mapping approach. *Nucleic Acids Research* **41**: e129-e129.

He L, Qian J, Li X, Sun ZY, Xu XL, Chen SL. 2017. Complete Chloroplast Genome of Medicinal Plant *Lonicera japonica*: Genome Rearrangement, Intron Gain and Loss, and Implications for Phylogenetic Studies. *Molecules* **22**: 249.

Hoang DT, Chernomor O. 2018. UFBoot2: improving the ultrafast bootstrap approximation. *Molecular Biology and Evolution* **35**: 518-522.

Hodel R, Zimmer EA, Wen J. 2021. A phylogenomic approach resolves the backbone of *Prunus* (Rosaceae) and identifies signals of hybridization and allopolyploidy. *Molecular Phylogenetics and Evolution* 107118.

Jacobs B, Pyck N, Smets E. 2010. Phylogeny of the Linnaea clade: are *Abelia* and *Zabelia* closely related?. *Molecular Phylogenetics and Evolution* **57**: 741-752.

Jiang XL, Hipp AL, Deng M, Su T, Zhou ZK, Yan MX. 2019. East Asian origins of European holly oaks (*Quercus* section *Ilex* Loudon) via the Tibet□Himalaya. *Journal of Biogeography* **46**: 2203-2214.

Jin WY, Li HW, Wei R, Huang BH, Liu B, Sun TT, Mabberley DJ, Liao PC, Yang Y. 2020. New insights into biogeographical disjunctions between Taiwan and the Eastern Himalayas: The case of *Prinsepia* (Rosaceae). *Taxon* **69**: 278-289.

Kalyaanamoorthy S, Minh BQ, Wong TK, Von Haeseler A, Jermiin LS. 2017. ModelFinder: fast model selection for accurate phylogenetic estimates. *Nature Methods* **14**: 587-589.

Katoh K, Standley DM. 2013. MAFFT multiple sequence alignment software version 7:

improvements in performance and usability. *Molecular Biology and Evolution* **30**: 772-780.

Kim TJ, Sun BY, Park CW, Suh Y. 1998. Phylogenetic implications of *matK* sequences in Caprifoliaceae. *American Journal of Botany* **48**: 1-48.

Landrein S, Buerki S, Wang HF, Clarkson JJ. 2017. Untangling the reticulate history of species complexes and horticultural breeds in *Abelia* (Caprifoliaceae). *Annals of Botany* **120**: 257-269.

Landrein S, Farjon A. 2020. A monograph of Caprifoliaceae: Linnaeeae. *Kew Bulletin* **74**: 1-197.

Lanfear R, Calcott B, Ho SYW, Guindon S. 2012. PartitionFinder: combined selection of partitioning schemes and substitution models for phylogenetic analyses. *Molecular Biology and Evolution* **29**: 1695-1701.

Lanier HC, Knowles LL. 2012. Is recombination a problem for species-tree analyses?. *Systematic Biology* **61**: 691-701.

Lee-Yaw JA, Grassa CJ, Joly S, Andrew RL, Rieseberg LH. 2019. An evaluation of alternative explanations for widespread cytonuclear discordance in annual sunflowers (*Helianthus*). New Phytologist **221**: 515-526.

Li J, Milne RI, Ru D, Miao J, Tao W, Zhang L, Mao K. 2000. Allopatric divergence and hybridization within *Cupressus chengiana* (Cupressaceae), a threatened conifer in the northern Hengduan Mountains of western China. *Molecular Ecology* **29**: 1250-1266.

Li HL, Keng H. 1950. Phytogeographical affinities of southern Taiwan. *Taiwania* **1**: 103-128.

Li R, Wen J. 2016. Phylogeny and diversification of Chinese Araliaceae based on nuclear and plastid DNA sequence data. *Journal of Systematics and Evolution* **54**: 453-467.

Liu YP, Ren ZM, Harris AJ, Peterson PM, Wen J, Su X. 2018. Phylogeography of *Orinus* (Poaceae), a dominant grass genus on the Qingha-Tibet Plateau. *Botanical Journal of the Linnean Society* **186**: 202-223.

Linder PH, Antonelli A, Humphreys AM, Pirie MD, Wüest RO. 2013. What determines biogeographical ranges? Historical wanderings and ecological constraints in the danthonioid grasses. *Journal of Biogeography* **40**: 821-834.

Link-Pérez MA, Dollo VH, Weber KM, Schussler EE. 2010. What's in a Name: Differential labelling of plant and animal photographs in two nationally syndicated elementary science textbook series. *International Journal of Science Education* **32**: 1227-1242.

López-Pujol J, Ren M. 2010. China: a hot spot of relict plant taxa. In: Rescigno, V., Maletta, S. (Eds.), Biodiversity hotspots. Nova Science Publishers, *New York* 123-137.

Lu SY, Peng CI, Cheng YP, Hong KH, Chiang TY. 2001. Chloroplast DNA phylogeography of *Cunninghamia konishii* (Cupressaceae), an endemic conifer of Taiwan. *Genome* **44**: 797-807.

Manchester SR. 2000. Update on the megafossil flora of Florissant, Colorado. *Denver Museum of Nature and Science* **4**:137-162.

Morales-Briones DF, Liston A, and Tank DC. 2018. Phylogenomic analyses reveal a deep history of hybridization and polyploidy in the Neotropical genus *Lachemilla* (Rosaceae). *New Phytologist* **218**: 1668-1684.

Morales-Briones DF, Gehrke B, Huang CH, Liston A, Ma H, Marx HE, Tank DC and Yang Y. 2021. Analysis of paralogs in target enrichment data pinpoints multiple ancient polyploidy events in *Alchemilla* s.l. (Rosaceae). *Systematic Biology* syab032.

Mummenhoff K, Linder P, Friesen N, Bowman JL, Lee JY, Franzke A. 2004. Molecular evidence for bicontinental hybridogenous genomic constitution in *Lepidium* sensu stricto (Brassicaceae) species from Australia and New Zealand. *American Journal of Botany* **91**: 254-261.

Nathan R, Schurr FM, Spiegel O, Steinitz O, Trakhtenbrot A, Tsoar A. 2008. Mechanisms of long-distance seed dispersal. *Trends in ecology evolution* **23**: 638-647.

Nguyen LT, Schmidt HA, von Haeseler A, Minh, BQ. 2015. IQ-TREE: a fast effective stochastic algorithm for estimating maximum-likelihood phylogenies. *Molecular Biology and Evolution* **32**: 268-274.

Nie ZL, Sun H, Li H, Wen J. 2007. Intercontinental biogeography of subfamily Orontioideae (*Symplocarpus*, *Lysichiton*, and *Orontium*) of Araceae in eastern Asia and North America. *Molecular Phylogenetics and Evolution* **40**: 155-165.

Niu YT, Ye JF, Zhang JL, Wan JZ, Yang T, Wei XX, Lu LM, Li JH, Chen ZD. 2018. Long-distance dispersal or postglacial contraction? Insights into disjunction between Himalayan-Hengduan Mountains and Taiwan Island in a cold-adapted herbaceous genus, *Triplostegia*. *Ecology and Evolution* **8**: 1131-1146.

Nosil P. 2008. Speciation with gene flow could be common. *Molecular ecology* **1**7: 2103-2106.

Nylander JAA, Ronquist F, Huelsenbeck JP, Nieves-Aldrey JL. 2004. Bayesian phylogenetic analysis of combined data. *Systematic Biology* **53**: 47-67.

Phillips SJ, Anderson RP, Schapire RE. 2006. Maximum entropy modeling of species geographic distributions. *Ecological Modelling* **190**: 231-259.

Qian H, Ricklefs RE. 2004. Geographical distribution and ecological conservatism of disjunct genera of vascular plants in eastern Asia and eastern North America. *Journal of Ecology* **92**: 253-265.

Qiu YX, Fu CX, Comes HP, 2011. Plant molecular phylogeography in China and adjacent regions: Tracing the genetic imprints of Quaternary climate and environmental change in the world's most diverse temperate flora. *Molecular Phylogenetics and Evolution* **59**: 225-244.

Rambaut A, Suchard MA, Xie D, Drummond AJ. 2014. Tracer, version 1.6. http://beast.bio.ed.ac.uk/Tracer/

Rehder A. 1911. Caprifoliaceae. In: Sargent C S ed. Plantae Wilsonianae. *Cambridge University Press*. **1**: 118-129.

Šarhanová P, Sharbel TF, Sochor M, Vašut RJ, Dančák M and Trávníček B. 2017. Hybridization drives evolution of apomicts in *Rubus* subgenus *Rubus*: evidence from microsatellite markers. *Annals of Botany* **120**: 317-328.

Schwarz G. 1978. Estimating the dimension of a model. *Annals of Statistics* **6**: 461-464

Shi Y, Cui Z, Su Z. 2006. The Quaternary glaciations and environmental variations in China. *Hebei Science and Technology Press* **65**: 101.

Sibuet JC, Hsu SK, Le Pichon X, Le Formal JP, Reed D, Morre G, Liu CS. 2002. East Asia plate tectonics since 15 Ma: constraints from the Taiwan Island region. *Tectonophysics* **344**: 103-134.

Sibuet JC, Hsu SK. 2004. How was Taiwan Island created?. *Tectonophysics* **379**: 159-181.

Smith SA, Dunn CW. 2008. Phyutility: a phyloinformatics tool for trees, alignments and molecular data. *Bioinformatics* **24**: 715-716.

Sugiura N. 1978. Further Analysis of the Data by Akaike's Information Criterion and the Finite Corrections. *Communications in Statistics-Theory and Methods* **7**: 13-26.

Suo YH, Li SZ, Zhao SJ, Somerville ID, Yu S, Dai LM, Xu LQ, Cao XZ, Wang PC. 2015. Continental margin basins in East Asia: tectonic implications of the Meso- Cenozoic East China Sea pull-apart basins. *Geological Journal* **50**: 139-156.

Swets JA. 1988. Measuring the accuracy of diagnostic systems. *Science* **240**: 1285-1293.

Teng LS. 1992. Geotectonic evolution of Tertiary continental margin basins of Taiwan. *Petroleum Geology of Taiwan Island* **27**: 1-19.

Vargas OM, Heuertz M, Smith SA, Dick CW. 2019. Target sequence capture in the Brazil nut family (Lecythidaceae): Marker selection and in silico capture from genome skimming data. *Molecular Phylogenetics and Evolution* **135**: 98-104.

Wallich N. 1829. *Plantae Asiaticae rariores*. London, Paris, Strasburgh: Treuttel and Würtz

Wang HF, Landrein S, Dong WP, Nie ZL, Kondo K, Funamoto T, Wen J, Zhou SL. 2015. Molecular phylogeny and biogeographic diversification of Linnaeoideae (*Carprifoliaceae s.l.*) disjunctively distributed in Eurasia, North American and Mexico. *PLoS One* **10**: e0116485.**Wang HX, Liu H, Moore MJ, Landrein S, Liu B, Zhu ZX, Wang HF. 2020a.** Plastid phylogenomic insights into the evolution of the Caprifoliaceae *s.l.* (Dipsacales). *Molecular Phylogenetics and Evolution* **142**: 106641.

Wang HX, Moore MJ, Barrett RL, Landrein S, Sakaguchi S, Maki M, Wen J, Wang HF.

2020b. Plastome phylogenomic insights into the Sino-Japanese biogeography of Diabelia (Caprifoliaceae). *Journal of Systematics and Evolution* **58:** 972-987.

Wang HX, Morales-Brionesb DF, Moorec MJ, Wen J, Wang HF. 2021. A phylogenomic perspective on gene tree conflict and character evolution in *Caprifoliaceae* using target enrichment data, with Zabelioideae recognized as a new subfamily. *Journal of Systematics and Evolution* **59:** 897-914.

Wang IJ. 2013. Examining the full effects of landscape heterogeneity on spatial genetic variation: a multiple matrix regression approach for quantifying geographic and ecological isolation. *Evolution* **67**: 3403-3411.

Wang J, Feng C, Jiao T, Von Wettberg EB, Kang M. 2017. Genomic Signature of Adaptive Divergence despite Strong Nonadaptive Forces on Edaphic Islands: A Case Study of *Primulina juliae*. *Genome Biology and Evolution* **9**: 3495-3508.

Wang W, Ortiz RDC, Jacques FM, Xiang XG, Li H., Lin L, Chen ZD. 2012. Menispermaceae and the diversification of tropical rainforests near the Cretaceous-Paleogene boundary. *New Phytologist* **195**: 470-478.

Wang Z, Liu KJ. 2016. A performance study of the impact of recombination on species tree analysis. *BMC Genomics* **17**: 165-174.

Wei XX, Yang ZY, Li Y, Wang XQ. 2010. Molecular phylogeny and biogeography of Pseudotsuga (Pinaceae): insights into the floristic relationship between Taiwan Island and its adjacent areas. *Molecular Phylogenetics and Evolution* **55**: 776-785.

Weitemier K, Straub SCK, Cronn RC, Fishbein M, Schmickl R, McDonnell A, Liston A. 2014. Hyb-Seq: combining target enrichment and genome skimming for plant phylogenomics. *Applications in Plant Sciences* **2**: 1400042.

Wen J. 2001. Evolution of eastern Asian-eastern North American biogeographic disjunctions: a few additional issues. *International Journal of Plant Sciences* **162**: S117-S122.

Wen J, Nie ZL, Ickert□Bond SM. 2018. Advances in biogeography in the age of a new modern synthesis. *Journal of Systematics and Evolution* **57**: 543-546.

Wen J, Ree RH, Ickert-Bond SM, Nie Z, Funk V. 2013. Biogeography: where do we go from here?. *Taxon* **62**: 912-927.

Wen J, Wagner WL. 2020. Collections-based systematics and biogeography in the 21st century. *Journal of Systematics and Evolution* **58**: 743-750.

Wu PC, Wang MZ. 2001. Relationship of the tropical elements of the bryophytes between Hengduan Mts., southwest China and Taiwan Island province, southeast China. *Guizhou Science* **19**: 6-9.

Xiang CL, Dong HJ, Landrein S, Zhao F, Yu WB, Soltis DE, Peng H. 1998. Revisiting the phylogeny of Dipsacales: new insights from phylogenomic analyses of complete plastomic sequences. *Journal of Systematics and Evolution* **58**: 103-117.

Xiang KL, Zhao L, Erst AS, Yu SX, Jabbour F, Wang W. 2017. A molecular phylogeny of *Dichocarpum* (Ranunculaceae): Implications for eastern Asian biogeography. *Molecular Phylogenetics and Evolution* **107**: 594-604.

Xiang QY, Soltis DE. 2001. Dispersal-vicariance analyses of intercontinental disjuncts: historical biogeographical implications for angiosperms in the Northern Hemisphere. *International Journal of Plant Sciences* **162**: S29-S39.

Xu J, Deng M, Jiang XL, Westwood M, Song YG, Turkington R. 2015. Phylogeography of *Quercus glauca* (Fagaceae), a dominant tree of East Asian subtropical evergreen forests, based on three chloroplast DNA interspace sequences. *Tree Genet Genomes* **11**: 805.

Yan HF, Zhang CY, Wang FY, Hu, CM, Ge XJ, Hao G. 2012. Population expanding with the phalanx model and lineages split by environmental heterogeneity: a case study of *Primula obconica* in subtropical China. *PLoS One* **7**: e41315.

Yang Q, Landrein S. 2011. *Linnaeaceae. Flora of China* **19**: 642-648.

Yang Y, Smith SA. 2014. Orthology inference in nonmodel organismsusing transcriptomes and low-coverage genomes: improving accuracy and matrix occupancy for phylogenomics. *Molecular Biology and Evolution* **31**: 3081-3092.

Ye J, Lu L, Liu B, Yang T, Zhang J, Hu H, Chen Z. 2019. Phylogenetic delineation of regional biota: A case study of the Chinese flora. *Molecular Phylogenetics and Evolution* **135**: 222-229.

Ye XQ. 1982. On the formation and development of the geology and geomorphology of Taiwan. *Journal Central China Teachers College* 83-89.

Ye XY, Ma PF, Yang GQ, Guo C, Zhang YX, Chen YM, Li DZ. 2019. Rapid diversification of alpine bamboos associated with the uplift of the Hengduan Mountains. *Journal of Biogeography* **46**: 2678-2689.

Ye Z, Zhu G, Chen P, Zhang D, Bu W. 2014. Molecular data and ecological niche modelling reveal the Pleistocene history of a semi-aquatic bug (*Microvelia douglasi douglasi*) in East Asia. *Molecular Ecology* **23**: 3080-3096.

Yin A, Harrison TM. 2000. Geologic evolution of the Himalayan Tibetan orogen. *Annual Review of Earth and Planetary Sciences* **28**: 211-280.

Ying T, Zhang Y, Boufford DE. 1994. The endemic genera of seed plants of China. Science press, Beijing.

Yoder AD, Nowak MD. 2006. Has vicariance or dispersal been the predominant biogeographic force in Madagascar? Only time will tell. *Ecology Evolution and Systematics* **37**: 405-431.

Yu Y, Harris AJ, Blair C, He X. 2015. RASP (Reconstruct Ancestral State in Phylogenies): a tool for historical biogeography. *Molecular Phylogenetics and Evolution* **87**: 46-49.

Zachos J, Pagani M, Sloan L, Thomas E, Billups K. 2001. Trends, rhythms, and aberrations in global climate 65 Ma to present. *Science* **292**: 686-693.

Zhang C, Rabiee M, Sayyari E, Mirarab S. 2018. ASTRAL-III: polynomial time species tree reconstruction from partially resolved gene trees. *BMC Bioinformatics* **19**: 15-30.

Figure Legends

Figure 1. Photographs of *Abelia* taxa. (A) *A. chinensis*; (B) *A. chinensis* var. *ionandra*; (C) *A. forrestii* (photograph by Sven Landrein); (D) *A.* × *grandiflora*; (E) *A.* × *grandiflora* ‘Francis Mason’ (photograph by Sven Landrein); (F) *A. macrotera*; (G) *A. macrotera*

var. *macrotera* (photograph by Sven Landrein); (H) *A. uniflora* (photograph by Pan Li); (I) *A. schumannii* (photograph by Sven Landrein).

Figure 2. Tanglegram of the nuclear concatenated (Left) and plastid (Right) phylogenies. Dotted lines connect taxa between the two phylogenies. The support values are shown above branches. The asterisks indicate maximum likelihood bootstrap support of 100%. Major taxonomic groups or main clades in the family as currently recognized are indicated by branch colors as a visual reference to relationships.

Figure 3. ASTRAL-III species tree; Clade support is depicted as: Quartet Concordance (QC)/Quartet Differential (QD)/Quarte Informativeness (QI)/Local posterior probabilities (LPP).

Figure 4. Best supported species networks inferred with PhyloNet for the (A) 15 samples, (B) 12 samples. Numbers next to the inferred hybrid branches indicate inheritance probabilities. Red lines represent minor hybrid edges (edges with an inheritance contribution < 0.50).

Figure 5. BEAST analysis of divergence times based on nuclear data. Calibration points are indicated by stars. Numbers 1-9 represent major divergence events in *Abelia*; Mean divergence times and 95% highest posterior densities are provided for each.

Figure 6. Ancestral area reconstruction for *Abelia*. Areas of endemism are as follows: (A) southwestern China, (B) central-eastern China, (C) Taiwan and Ryukyu islands. The numbered nodes represent crown nodes of important colonization events.

Figure 7. Comparison of potential distributions as probability of occurrence for *A. chinensis*, and *A. uniflora* at the CCSM climatic scenarios of the Last Glacial Maximum (LGM, ca. 21,000 years BP). The maximum training sensitivity plus specificity logistic threshold has been used to discriminate between suitable (cutline 0.1-1 areas) and unsuitable habitat. The darker color indicates a higher probability of occurrence.

Fig. S1 Heatmaps showing gene recovery efficiency for the nuclear gene in 45 species of *Abelia*. Columns represent genes, and each row is one accession. Shading indicates the percentage of the reference locus length coverage.

Fig. S2 Nuclear concatenated IQ-tree; Clade support is depicted as: Quartet Concordance (QC)/Quartet Differential (QD)/Quarte Informativeness (QI).

Fig. S3 Plastid IQ-tree; Clade support is depicted as: Quartet Concordance (QC)/Quartet Differential (QD)/Quarte Informativeness (QI)/Local posterior probabilities (LPP).

Fig. S4 Best species networks of the selective nuclear data estimated with PhyloNet for the 15 samples data set. A: One hybridization event; B: Two hybridization events; C: Three hybridization events; D: Four hybridization events; E: Five hybridization events. Blue branches connect the hybrid nodes. Numbers next to blue branches indicate inheritance probabilities.

Fig. S5 Best species networks of the selective nuclear data estimated with PhyloNet for the 12 samples data set. A: One hybridization event; B: Two hybridization events; C: Three hybridization events; D: Four hybridization events; E: Five hybridization events. Blue branches connect the hybrid nodes. Numbers next to blue branches indicate inheritance probabilities.

Fig. S6 BEAST analysis of divergence times based on the plastid matrix. Calibration points are indicated by stars. Numbers 1-8 represent major divergence events in *Abelia*; Mean divergence times and 95% highest posterior densities are provided for each.

Fig. S7 Potential distribution probability (in logistic value) of occurrence for *Abelia* in East Asia generated form MAXENT.

Table. S1 The 19 bioclimatic variables for ENM analyses.

Table. S2 HybPiper assembly statistics.

Table 1. **List of species and vouchers used in this study.**

Order	Ingroup/ Outgroup	Taxon	Coding	Locality	Voucher specimen number	Serial number	SRA accession
1	Ingroup	*Abelia chinensis*	B	Jiujiang, Jiangxi, China	HUTB, E119	E119	SRR13890741
2	Ingroup	*Abelia chinensis*	B	Jiujiang, Jiangxi, China	HUTB, E111	E111	SRR13890742
3	Ingroup	*Abelia chinensis*	B	Jiujiang, Jiangxi, China	HUTB, E206	E206	SRR13705765
4	Ingroup	*Abelia chinensis* var. *ionandra*	C	Keelung Islet,Taiwan, China	HUTB, E30	E30	SRR13705776
5	Ingroup	*Abelia chinensis* var. *ionandra*	C	Amami Islands, Japan	HUTB, E33	E33	SRR13890725
6	Ingroup	*Abelia chinensis* var. *ionandra*	C	Okinawa Island, Okinawa, Japan	HUTB, E166	E166	SRR13890726
7	Ingroup	*Abelia chinensis* var. *ionandra*	C	Yilan, Taiwan, China	HUTB, E167	E167	SRR13890744
8	Ingroup	*Abelia chinensis* var. *ionandra*	C	Yilan,Taiwan, China	HUTB, E229	E229	SRR13890743
9	Ingroup	*Abelia chinensis* var. *ionandra*	C	Yilan, Taiwan, China	HUTB, E230	E230	SRR13890751
10	Ingroup	*Abelia chinensis* var. *ionandra*	C	Yilan, Taiwan, China	HUTB, E231	E231	SRR13890745
11	Ingroup	*Abelia forrestii*	A	Nujiang, Yunnan, China	HUTB, E36	E36	SRR13890748
12	Ingroup	*Abelia forrestii*	A	Nujiang, Yunnan, China	K, 2051	E37	SRR13705787
13	Ingroup	*Abelia grandiflora*	B	Zhengzhou, Henan, China	HUTB, E159	E159	SRR13890724
14	Ingroup	*Abelia grandiflora*	B	Zhengzhou, Henan, China	HUTB, E227	E227	SRR13890730
15	Ingroup	*Abelia macrotera* var. *mairei*	A	Liangshan,Sichuan, China	HUTB, E110	E110	SRR13705799
16	Ingroup	*Abelia macrotera* var. *deutziaefolia*	A	Fuyang, Guizhou, China	HUTB, E153	E153	SRR13890758
17	Ingroup	*Abelia macrotera* var. *deutziaefolia*	A	Fuyang, Guizhou, China	HUTB, E154	E154	SRR13890757
18	Ingroup	*Abelia macrotera* var. *deutziaefolia*	A	Fuyang, Guizhou, China	HUTB, E155	E155	SRR13890727
19	Ingroup	*Abelia macrotera* var. *deutziaefolia*	A	Fuyang, Guizhou, China	HUTB, E156	E156	SRR13890731
20	Ingroup	*Abelia macrotera* var. *deutziaefolia*	A	Fuyang, Guizhou, China	HUTB, E157	E157	SRR13890728
21	Ingroup	*Abelia macrotera* var. *deutziaefolia*	A	Fuyang, Guizhou, China	HUTB, E158	E158	SRR13890729
22	Ingroup	*Abelia macrotera* var. *engleriana*	A	Nanchuan, Chongqing, China	HUTB, E34	E34	SRR13890756
23	Ingroup	*Abelia macrotera* var. *engleriana*	A	Nanchuan, Chongqing, China	HUTB, E149	E149	SRR13890753
24	Ingroup	*Abelia macrotera* var. *engleriana*	A	Nanchuan, Chongqing, China	HUTB, E347	E347	SRR13890755

25	Ingroup	*Abelia macrotera* var. *engleriana*	A	Nanchuan, Chongqing, China	HUTB, E349	E349	SRR13890754
26	Ingroup	*Abelia macrotera* var. *zabelioides*	A	Emei, Sichuan, China	HUTB, E3	E3	SRR13890733
27	Ingroup	*Abelia macrotera* var. *zabelioides*	A	Emei, Sichuan, China	HUTB, E43	E43	SRR13890740
28	Ingroup	*Abelia macrotera* var. *zabelioides*	A	Emei, Sichuan, China	HUTB, E211	E211	SRR13890732
29	Ingroup	*Abelia macrotera* var. *macrotera*	A	Yichang, Hubei, China	HUTB, E6	E6	SRR13890752
30	Ingroup	*Abelia macrotera* var. *macrotera*	A	Yichang, Hubei, China	HUTB, E45	E45	SRR13890750
31	Ingroup	*Abelia macrotera* var. *schumannii*	A	Ganzi, Sichuan, China	K, 2057	E44	SRR13890749
32	Ingroup	*Abelia uniflora*	B	Wuyishan, Fujian, China	HUTB, E46		SRR13890738
33	Ingroup	*Abelia uniflora*	B	Wuyishan, Fujian, China	HUTB, E47		SRR13890739
34	Ingroup	*Abelia uniflora*	B	Wuyishan, Fujian, China	HUTB, E48		SRR13890734
35	Ingroup	*Abelia uniflora*	B	Wuyishan, Fujian, China	HUTB, E51		SRR13705798
36	Ingroup	*Abelia uniflora*	B	Wuyishan, Fujian, China	HUTB, E52		SRR13890736
37	Ingroup	*Abelia uniflora*	B	Wuyishan, Fujian, China	HUTB, E53		SRR13890735
38	Ingroup	*Abelia uniflora*	B	Wuyishan, Fujian, China	HUTB, E54		SRR13890737
39	Outgroup	*Diabelia serrata*		Takakuma, Kagoshima, Japan	HUTB, E321		SRR13890747
40	Outgroup	*Diabelia sanguinea*		Numadzu, Shizuoka, Japan	HUTB, E303		SRR13890746
41	Outgroup	*Dipelta floribunda*		Cambridge, UK.	HUTB, E55		SRR13705794
42	Outgroup	*Dipelta floribunda*		Cambridge, UK.	HUTB, E56		SRR13705795
43	Outgroup	*Kolkwitzia amabilis*		Weinan, Shanxi, China	HUTB, E9		SRR13705797
44	Outgroup	*Linnaea borealis*		Yili, Xinjiang, China	HUTB, E14		SRR13705786
45	Outgroup	*Vesalea occidentalis*		Durango, Mexico	HUTB, E96		SRR13705793

Table 2. Dataset statistics, including the number of samples, number of characters, number of PI characters, missing data.

Alignment	No. of samples	No. sites	Missing data (%)	No. of variable/Parsimony informative sites
Nuclear	45	365,330	16.88	43,248/22,045
Plastid	45	163,130	4.35	7,926/3,850

Table 3. Model selection of the different species networks and bifurcating trees.

Topology	lnL	Parameters	Loci	Number of hybridizations	Information criteria		
					AIC	AICc	BIC
			15 samples				
nuclear ASTRAL	-4177.949631	27	167	N/A	8409.899262	8420.776960	8494.085095
nuclear IQ-TREE	-4148.054160	27	167	N/A	8350.108319	8360.986017	8434.294152
Plastid	-4231.190608	27	167	N/A	8516.381215	8527.258913	8600.567048
Network 1	-4088.228145	29	167	1	8234.456290	8247.157020	8324.878111
Network 2	-4050.799135	31	167	2	8163.598270	8178.294566	8260.256078
Network 3	-3948.351402	33	167	3	7962.702804	7979.574984	8065.596600
Network 4	**-3932.455932**	**35**	**167**	**4**	**7934.911864**	**7954.148505**	**8044.041647**
Network 5	-3935.844300	37	167	5	7945.688601	7967.487050	8061.054372
			12 samples				
nuclear ASTRAL	-2716.350474	21	162	N/A	5474.700949	5481.300949	5539.540472
nuclear IQ-TREE	-2724.448876	21	162	N/A	5490.897753	5497.497753	5555.737276
Plastid	-2723.043552	21	162	N/A	5488.087104	5494.687104	5552.926627
Network1	-2660.433072	23	162	1	5366.866143	5374.866143	5437.880859
Network2	-2601.023466	25	162	2	5252.046932	5261.605756	5329.236841
Network3	**-2549.319250**	**27**	**162**	**3**	**5152.638500**	**5163.922082**	**5236.003601**
Network4	-2552.995453	27	162	3	5159.990906	5171.274488	5243.356007
Network 5	-2606.591029	27	162	3	5267.182058	5278.465640	5350.547159

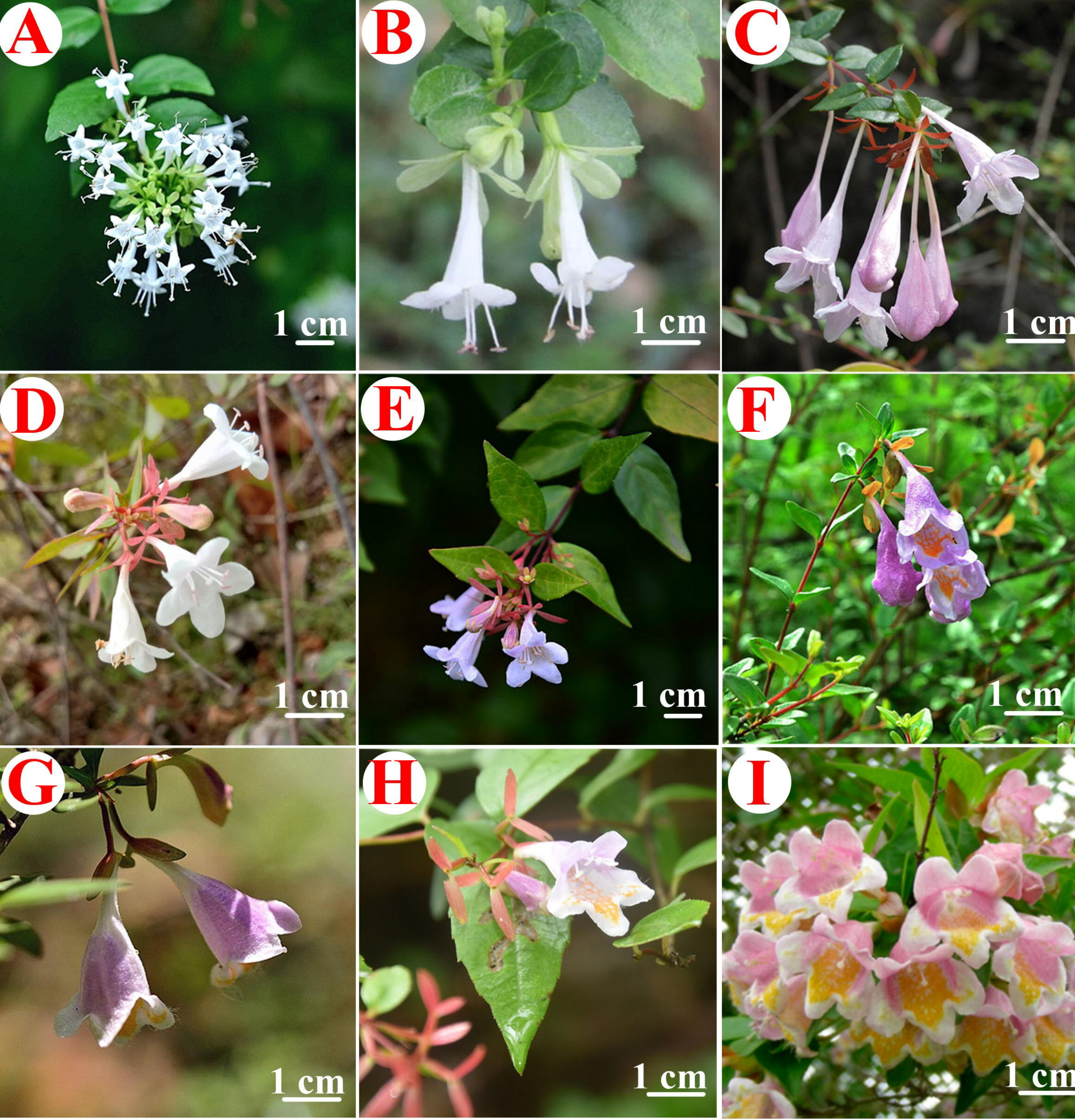
A
1 cm
B
1 cm
C
1 cm
D
1 cm
E
1 cm
F
1 cm
G
1 cm
H
1 cm
I
1 cm

Nuclear concatenated
Plastome
A. chinensis
A. uniflora
A. macrotera
A. forrestii
Outgroup
A. chinensis var. ionandra E231
A. chinensis var. ionandra E230
A. chinensis var. ionandra E167
A. chinensis var. ionandra E30
A. chinensis var. ionandra E229
A. chinensis var. ionandra E166
A. chinensis var. ionandra E33
A. chinensis E111
A. chinensis E119
A. chinensis E206
A. × grandiflora E227
A. × grandiflora E159
A. uniflora E47
A. uniflora E46
A. uniflora E54
A. uniflora E53
A. uniflora E52
A. uniflora E51
A. uniflora E48
A. macrotera var. zabelioides E3
A. macrotera var. zabelioides E43
A. macrotera var. zabelioides E211
A. macrotera var. deutziaefolia E157
A. macrotera var. deutziaefolia E156
A. macrotera var. deutziaefolia E158
A. macrotera var. deutziaefolia E155
A. macrotera var. engleriana E347
A. macrotera var. engleriana E349
A. macrotera var. engleriana E149
A. macrotera var. deatziaefolia E154
A. macrotera var. deatziaefolia E153
A. macrotera var. engleriana E34
A. macrotera var. macrotera E6
A. macrotera var. macrotera E45
A. macrotera var. schumannii E44
A. macrotera var. mairei E110
A. forrestii E36
A. forrestii E37
Diabelia sanguinea E303
D. serrata E321
Kolkwitzia amabilis E9
Dipelta floribunda E55
D. floribunda E56
Vesalea occidentalis E96
Linnaea borealis E14
99
81
77
89
96
86
83
95
97
98
82
89
84
91

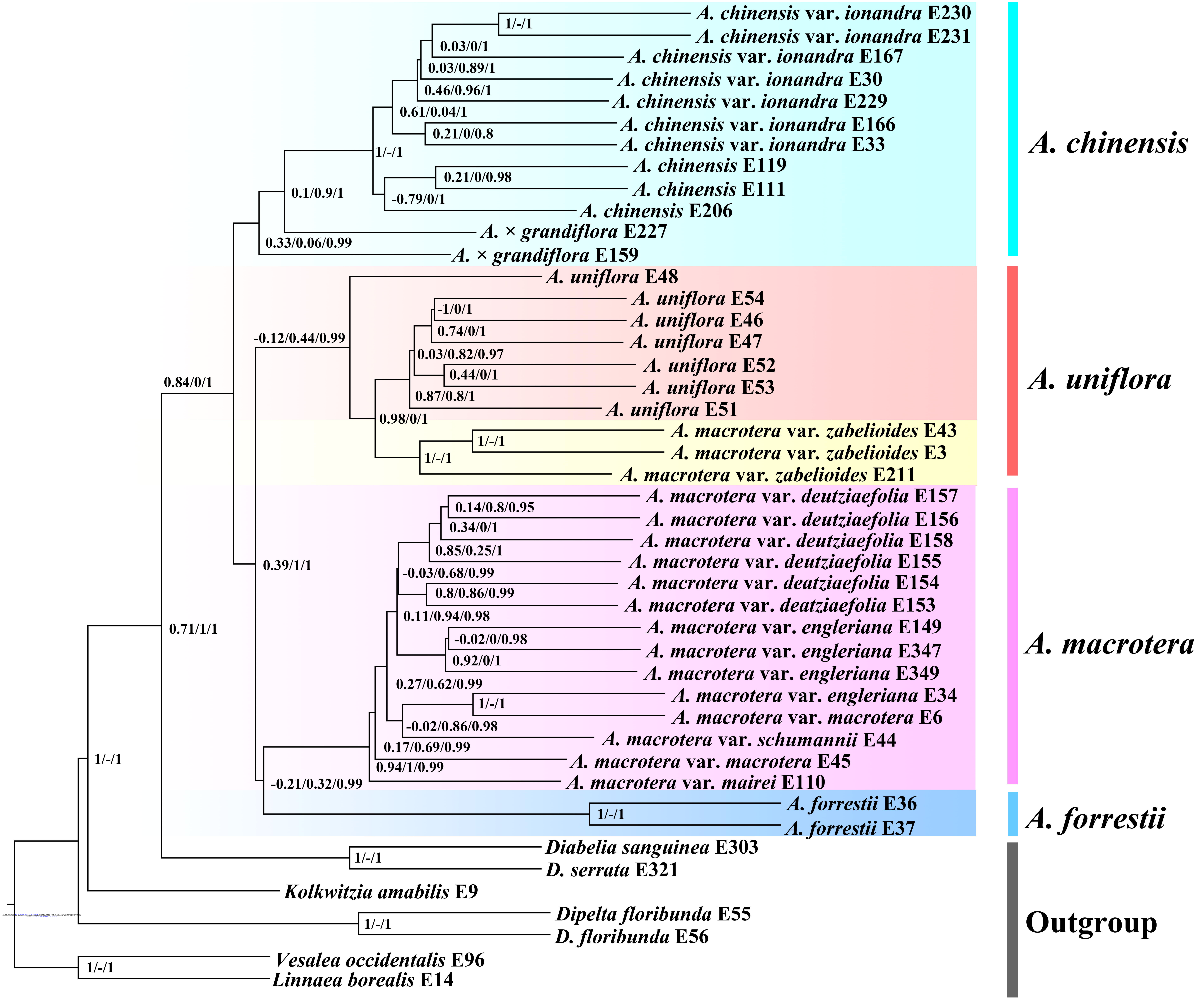
A. chinensis var. *ionandra* E230
1/-/1
A. chinensis var. *ionandra* E231
0.03/0/1
A. chinensis var. *ionandra* E167
0.03/0.89/1
A. chinensis var. *ionandra* E30
0.46/0.96/1
A. chinensis var. *ionandra* E229
0.61/0.04/1
A. chinensis var. *ionandra* E166
0.21/0/0.8
A. chinensis var. *ionandra* E33
1/-/1
A. chinensis E119
0.21/0/0.98
A. chinensis E111
0.1/0.9/1
-0.79/0/1
A. chinensis E206
A. × *grandiflora* E227
0.33/0.06/0.99
A. × *grandiflora* E159
A. chinensis
A. uniflora E48
A. uniflora E54
-1/0/1
A. uniflora E46
0.74/0/1
A. uniflora E47
-0.12/0.44/0.99
0.03/0.82/0.97
A. uniflora E52
0.44/0/1
A. uniflora E53
0.84/0/1
0.87/0.8/1
A. uniflora E51
0.98/0/1
A. uniflora
A. macrotera var. *zabelioides* E43
1/-/1
A. macrotera var. *zabelioides* E3
1/-/1
A. macrotera var. *zabelioides* E211
A. macrotera var. *deutziaefolia* E157
0.14/0.8/0.95
A. macrotera var. *deutziaefolia* E156
0.34/0/1
A. macrotera var. *deutziaefolia* E158
0.85/0.25/1
A. macrotera var. *deutziaefolia* E155
0.39/1/1
-0.03/0.68/0.99
A. macrotera var. *deatziaefolia* E154
0.8/0.86/0.99
A. macrotera var. *deatziaefolia* E153
0.11/0.94/0.98
A. macrotera var. *engleriana* E149
0.71/1/1
-0.02/0/0.98
A. macrotera var. *engleriana* E347
0.92/0/1
A. macrotera var. *engleriana* E349
0.27/0.62/0.99
A. macrotera var. *engleriana* E34
1/-/1
A. macrotera var. *macrotera* E6
-0.02/0.86/0.98
A. macrotera var. *schumannii* E44
0.17/0.69/0.99
A. macrotera var. *macrotera* E45
1/-/1
0.94/1/0.99
-0.21/0.32/0.99
A. macrotera var. *mairei* E110
A. macrotera
A. forrestii E36
1/-/1
A. forrestii E37
A. forrestii
Diabelia sanguinea E303
1/-/1
D. serrata E321
Kolkwitzia amabilis E9
Dipelta floribunda E55
1/-/1
D. floribunda E56
Outgroup
Vesalea occidentalis E96
1/-/1
Linnaea borealis E14

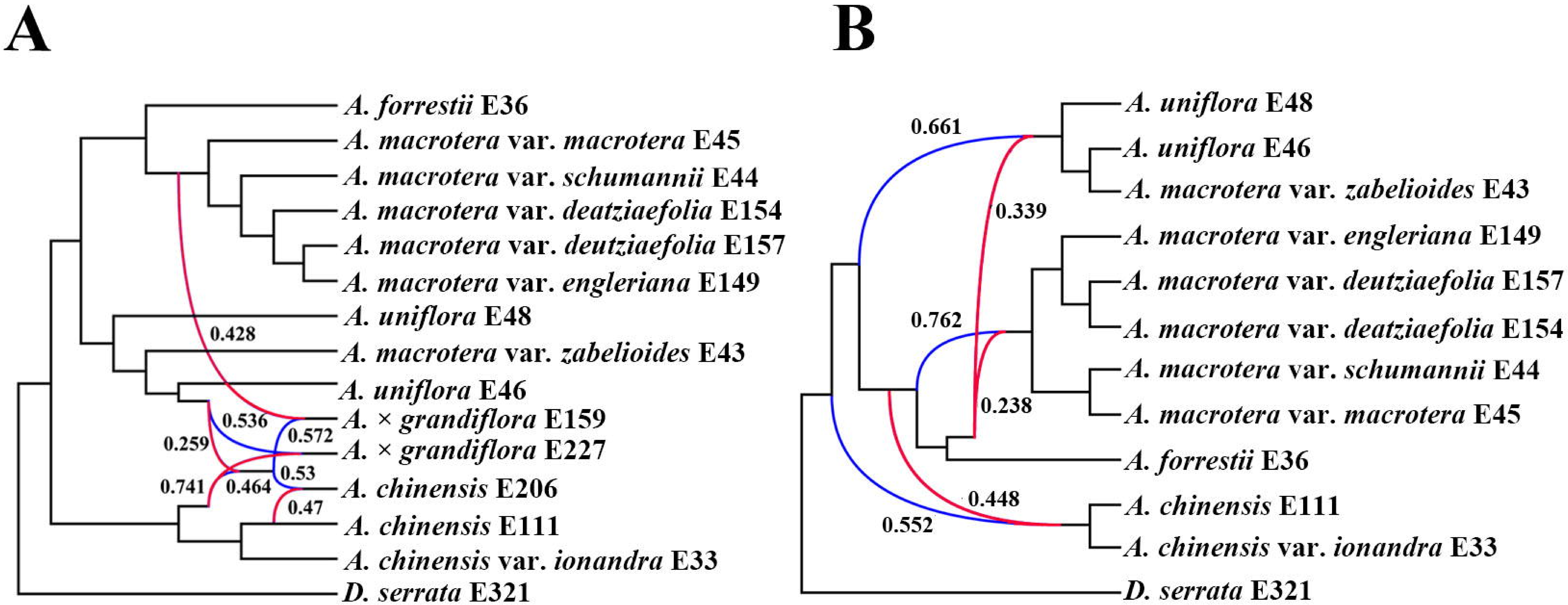
A
A. forrestii E36
A. macrotera var. macrotera E45
A. macrotera var. schumannii E44
A. macrotera var. deatziaefolia E154
A. macrotera var. deutziaefolia E157
A. macrotera var. engleriana E149
A. uniflora E48
0.428
A. macrotera var. zabelioides E43
A. uniflora E46
0.536
A. × grandiflora E159
0.572
0.259
A. × grandiflora E227
0.53
0.741
0.464
A. chinensis E206
0.47
A. chinensis E111
A. chinensis var. ionandra E33
D. serrata E321
B
0.661
A. uniflora E48
A. uniflora E46
A. macrotera var. zabelioides E43
0.339
A. macrotera var. engleriana E149
A. macrotera var. deutziaefolia E157
0.762
A. macrotera var. deatziaefolia E154
A. macrotera var. schumannii E44
0.238
A. macrotera var. macrotera E45
A. forrestii E36
0.448
A. chinensis E111
0.552
A. chinensis var. ionandra E33
D. serrata E321

★ 51.8 Ma
★ 36.0 Ma
❶ 33.47 [23.53 - 38.21] Ma
❷ 29.56 [21.64 - 33.76] Ma
❸ 24.93 [18.62 - 29.16] Ma
❹ 23.51 [16.91 - 27.09] Ma
❺ 18.53 [11.57 - 21.26] Ma
❻ 14.93 [12.39 - 20.21] Ma
❼ 12.44 [8.61 - 17.03] Ma
❽ 11.68 [7.99 - 15.13] Ma
❾ 6.24 [4.32 - 9.72] Ma
A. macrotera var. deatziaefolia E154
A. macrotera var. deatziaefolia E153
A. macrotera var. macrotera E45
A. macrotera var. schumannii E44
A. macrotera var. macrotera E6
A. macrotera var. engleriana E34
A. macrotera var. deutziaefolia E158
A. macrotera var. deutziaefolia E157
A. macrotera var. deutziaefolia E156
A. macrotera var. deutziaefolia E155
A. macrotera var. engleriana E347
A. macrotera var. engleriana E149
A. macrotera var. engleriana E349
A. macrotera var. mairei E110
A. uniflora E48
A. uniflora E53
A. uniflora E52
A. uniflora E54
A. uniflora E47
A. uniflora E46
A. uniflora E51
A. macrotera var. zabelioides E3
A. macrotera var. zabelioides E43
A. macrotera var. zabelioides E211
A. forrestii E36
A. forrestii E37
A. chinensis var. ionandra E167
A. chinensis var. ionandra E231
A. chinensis var. ionandra E230
A. chinensis var. ionandra E30
A. chinensis var. ionandra E229
A. chinensis var. ionandra E33
A. chinensis var. ionandra E166
A. chinensis E119
A. chinensis E111
A. chinensis E206
Diabelia sanguinea E303
D. serrata E321
Kolkwitzia amabilis E9
Dipelta floribunda E55
D. floribunda E56
Linnaea borealis E14
Vesalea occidentalis E96
1
2
3
4
5
6
7
8
9
6.0
Eocene
Oligocene
Miocene
Pli
Ple
50
40
30
20
10
0
Ma

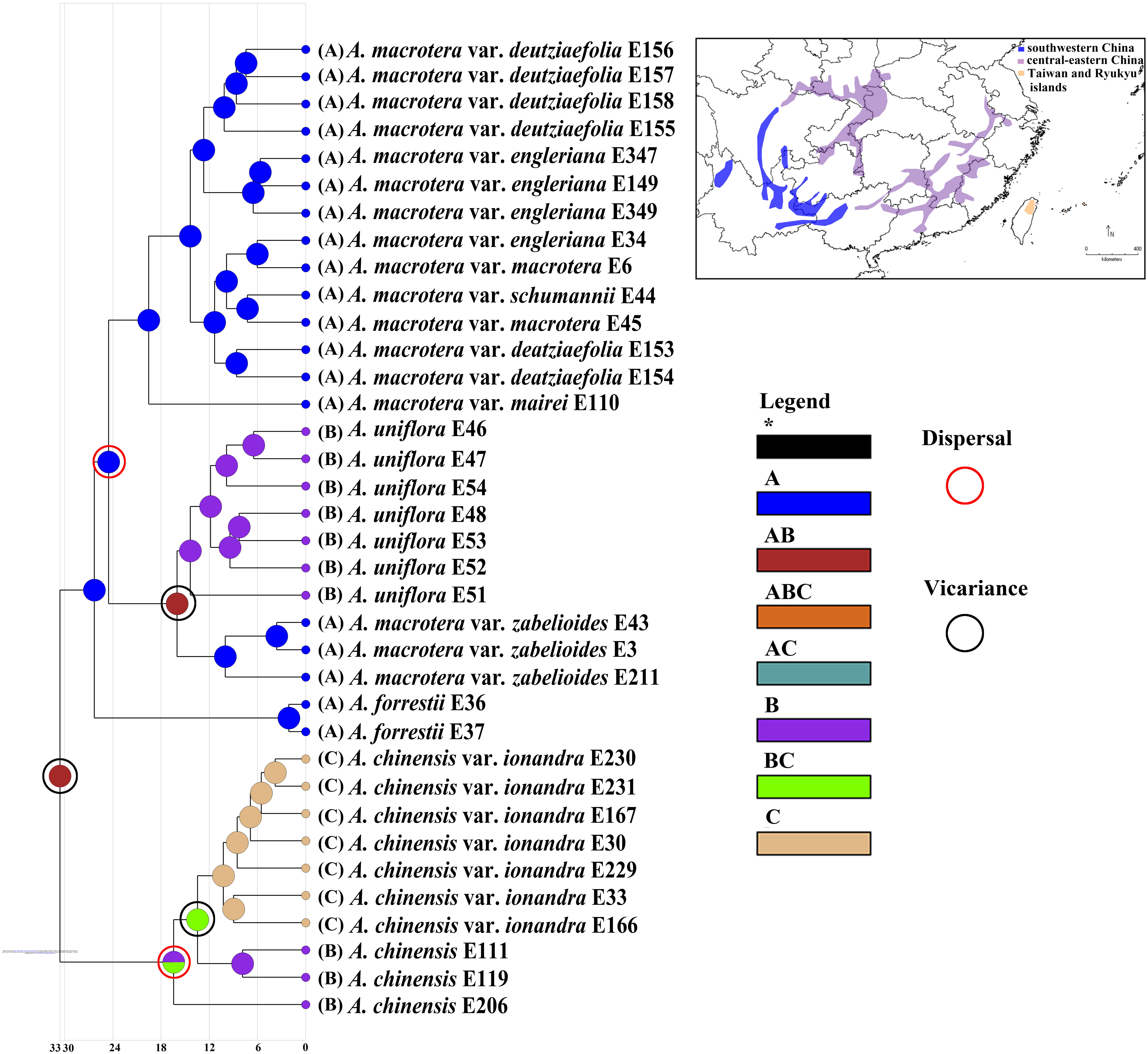
(A) A. macrotera var. deutziaefolia E156
(A) A. macrotera var. deutziaefolia E157
(A) A. macrotera var. deutziaefolia E158
(A) A. macrotera var. deutziaefolia E155
(A) A. macrotera var. engleriana E347
(A) A. macrotera var. engleriana E149
(A) A. macrotera var. engleriana E349
(A) A. macrotera var. engleriana E34
(A) A. macrotera var. macrotera E6
(A) A. macrotera var. schumannii E44
(A) A. macrotera var. macrotera E45
(A) A. macrotera var. deatziaefolia E153
(A) A. macrotera var. deatziaefolia E154
(A) A. macrotera var. mairei E110
(B) A. uniflora E46
(B) A. uniflora E47
(B) A. uniflora E54
(B) A. uniflora E48
(B) A. uniflora E53
(B) A. uniflora E52
(B) A. uniflora E51
(A) A. macrotera var. zabelioides E43
(A) A. macrotera var. zabelioides E3
(A) A. macrotera var. zabelioides E211
(A) A. forrestii E36
(A) A. forrestii E37
(C) A. chinensis var. ionandra E230
(C) A. chinensis var. ionandra E231
(C) A. chinensis var. ionandra E167
(C) A. chinensis var. ionandra E30
(C) A. chinensis var. ionandra E229
(C) A. chinensis var. ionandra E33
(C) A. chinensis var. ionandra E166
(B) A. chinensis E111
(B) A. chinensis E119
(B) A. chinensis E206
33 30 24 18 12 6 0
southwestern China
central-eastern China
Taiwan and Ryukyu islands
N
0 400
kilometers
Legend
*
A
AB
ABC
AC
B
BC
C
Dispersal
Vicariance

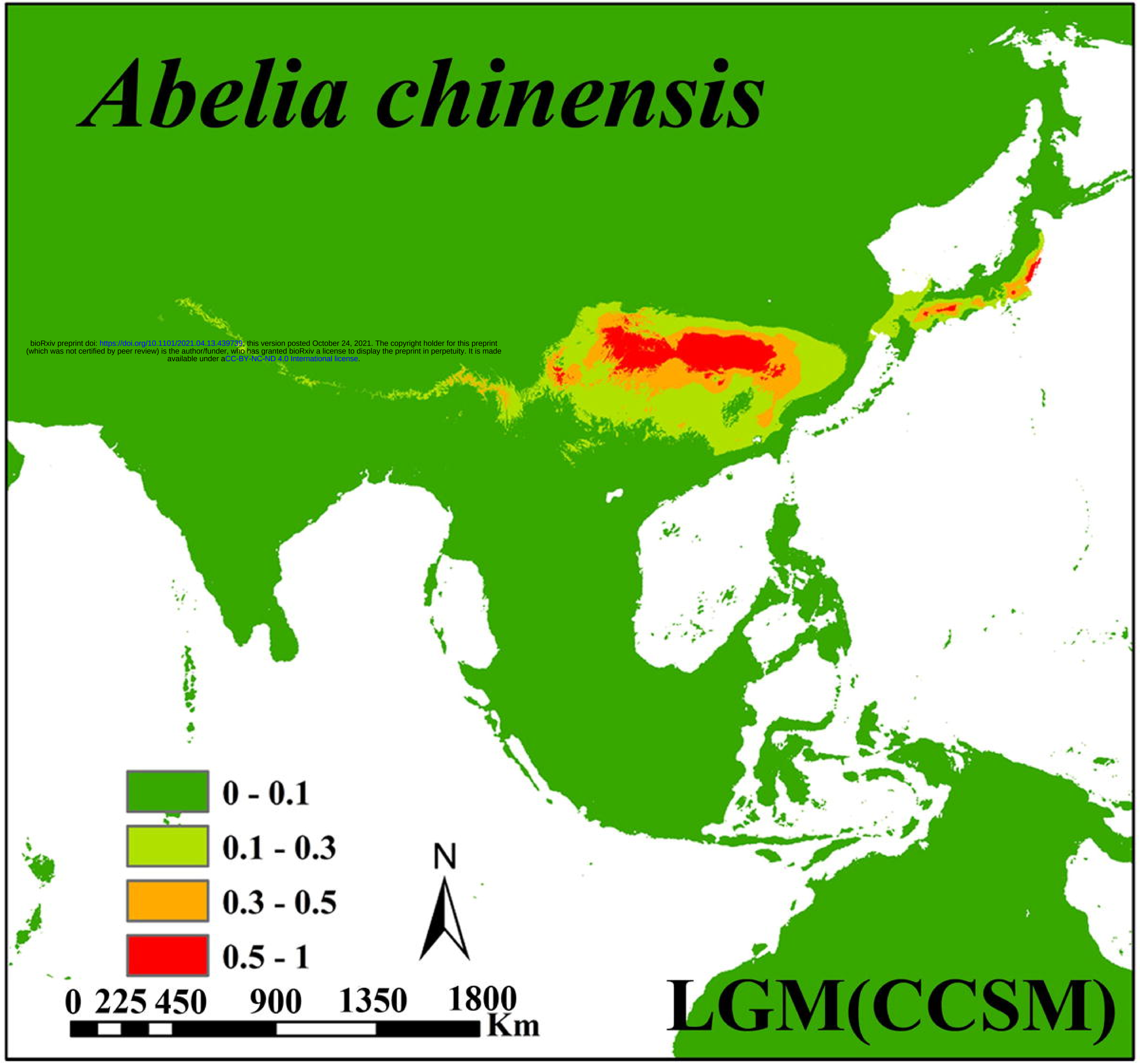
Abelia chinensis
🟩 0 - 0.1
🟩 0.1 - 0.3
🟧 0.3 - 0.5
🟥 0.5 - 1
N
0 225 450 900 1350 1800
Km
LGM(CCSM)

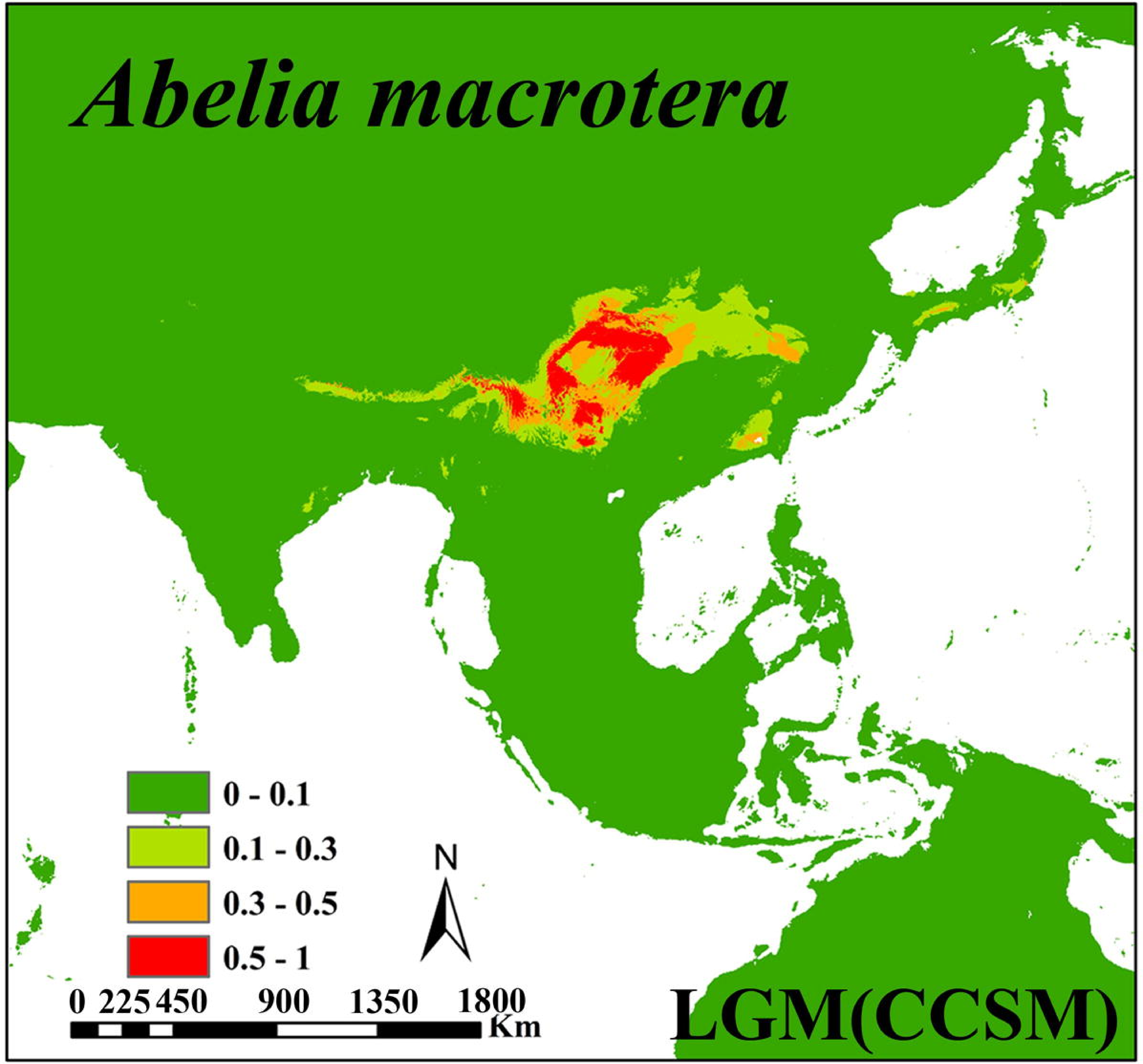
Abelia macrotera
🟩 0 - 0.1
🟩 0.1 - 0.3
🟧 0.3 - 0.5
🟥 0.5 - 1
N
0 225 450 900 1350 1800
Km
LGM(CCSM)

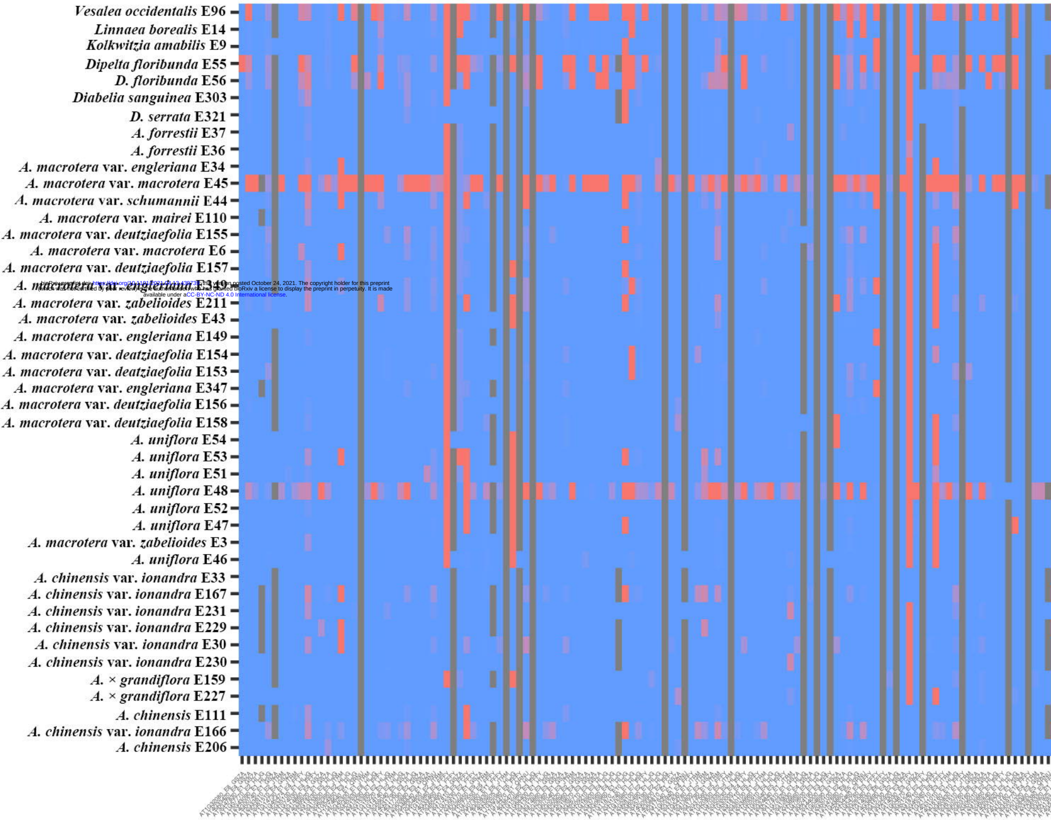
Vesalea occidentalis E96
Linnaea borealis E14
Kolkwitzia amabilis E9
Dipelta floribunda E55
D. floribunda E56
Diabelia sanguinea E303
D. serrata E321
A. forrestii E37
A. forrestii E36
A. macrotera var. *engleriana* E34
A. macrotera var. *macrotera* E45
A. macrotera var. *schumannii* E44
A. macrotera var. *mairei* E110
A. macrotera var. *deutziaefolia* E155
A. macrotera var. *macrotera* E6
A. macrotera var. *deutziaefolia* E157
A. macrotera var. *engleriana* E349
A. macrotera var. *zabelioides* E211
A. macrotera var. *zabelioides* E43
A. macrotera var. *engleriana* E149
A. macrotera var. *deatziaefolia* E154
A. macrotera var. *deatziaefolia* E153
A. macrotera var. *engleriana* E347
A. macrotera var. *deutziaefolia* E156
A. macrotera var. *deutziaefolia* E158
A. uniflora E54
A. uniflora E53
A. uniflora E51
A. uniflora E48
A. uniflora E52
A. uniflora E47
A. macrotera var. *zabelioides* E3
A. uniflora E46
A. chinensis var. *ionandra* E33
A. chinensis var. *ionandra* E167
A. chinensis var. *ionandra* E231
A. chinensis var. *ionandra* E229
A. chinensis var. *ionandra* E30
A. chinensis var. *ionandra* E230
A. × *grandiflora* E159
A. × *grandiflora* E227
A. chinensis E111
A. chinensis var. *ionandra* E166
A. chinensis E206

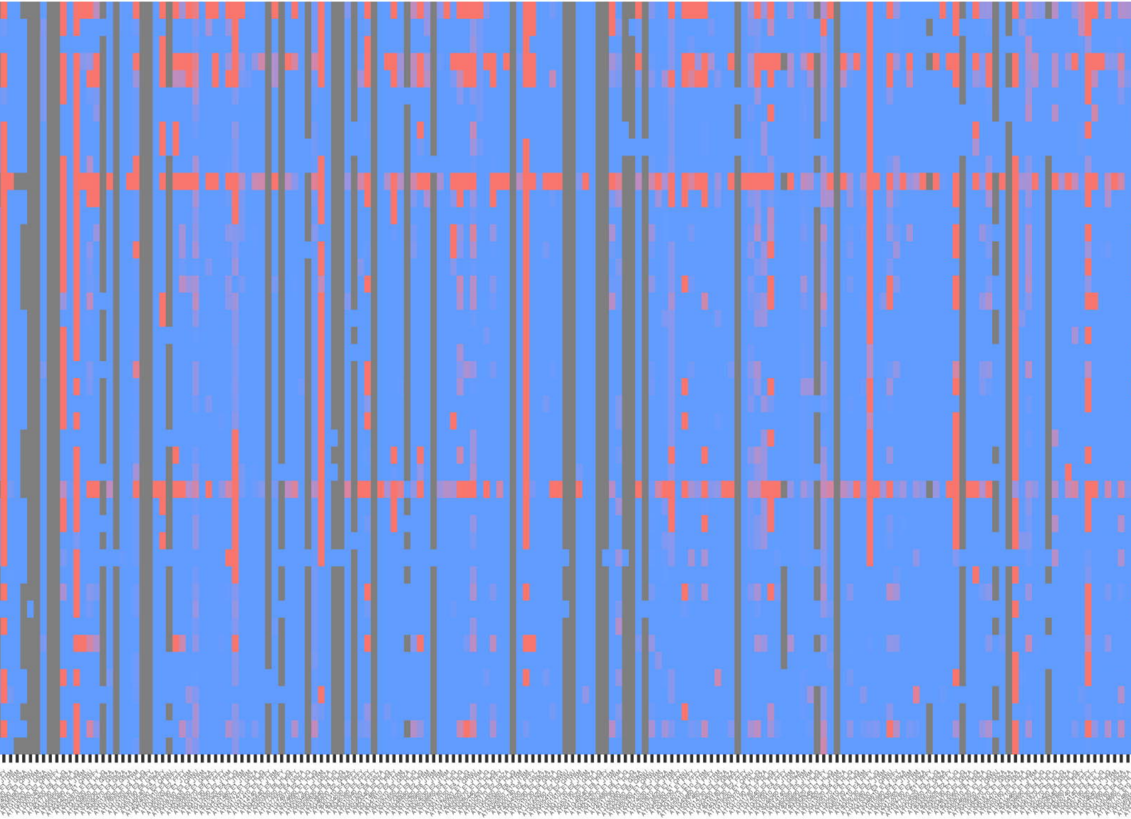

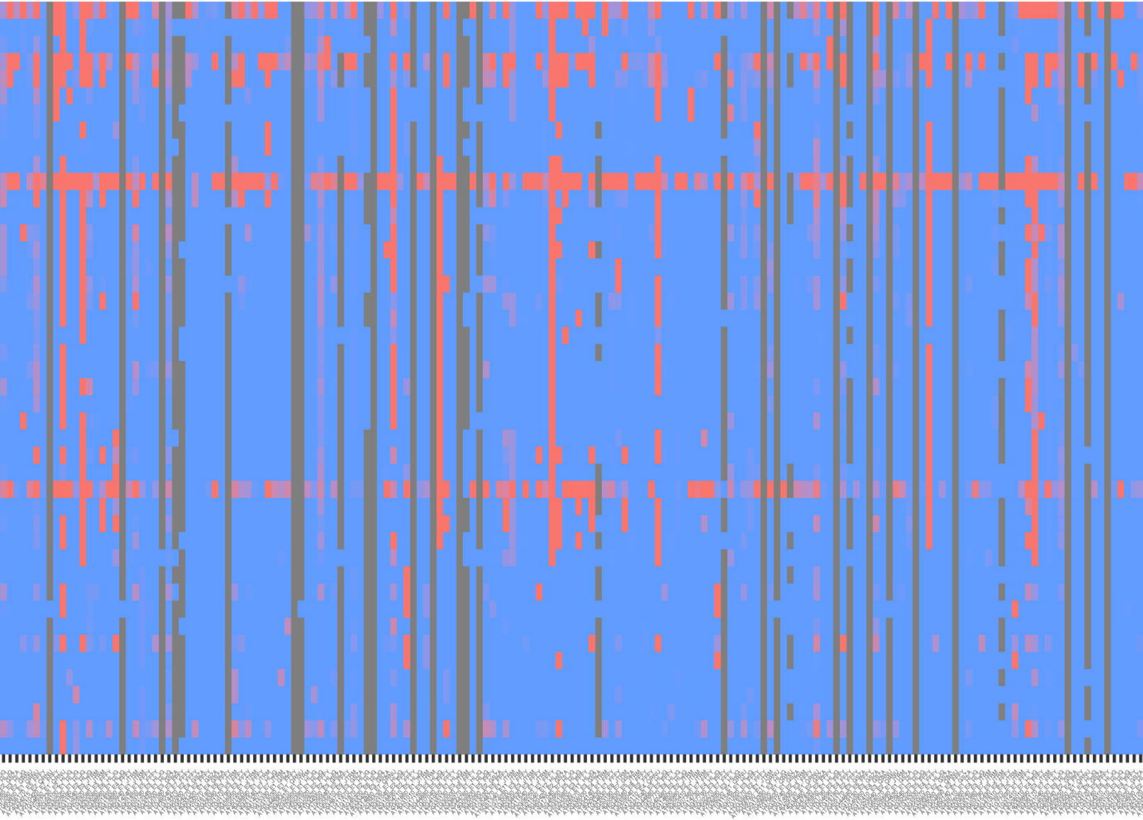

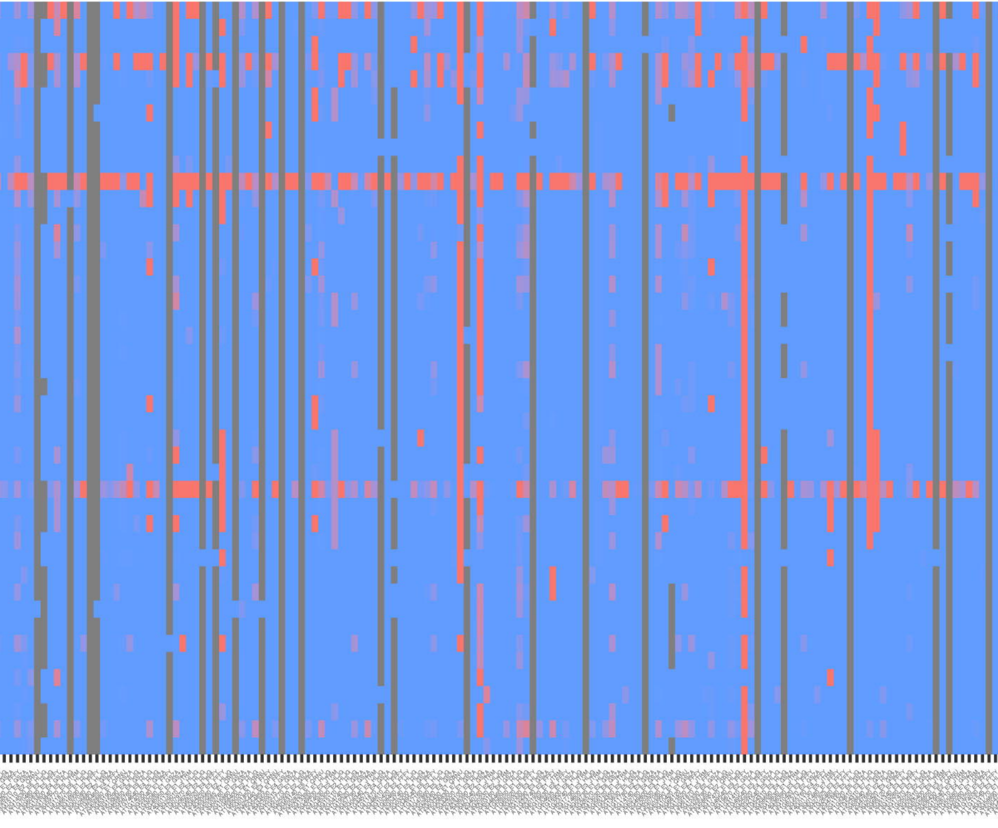

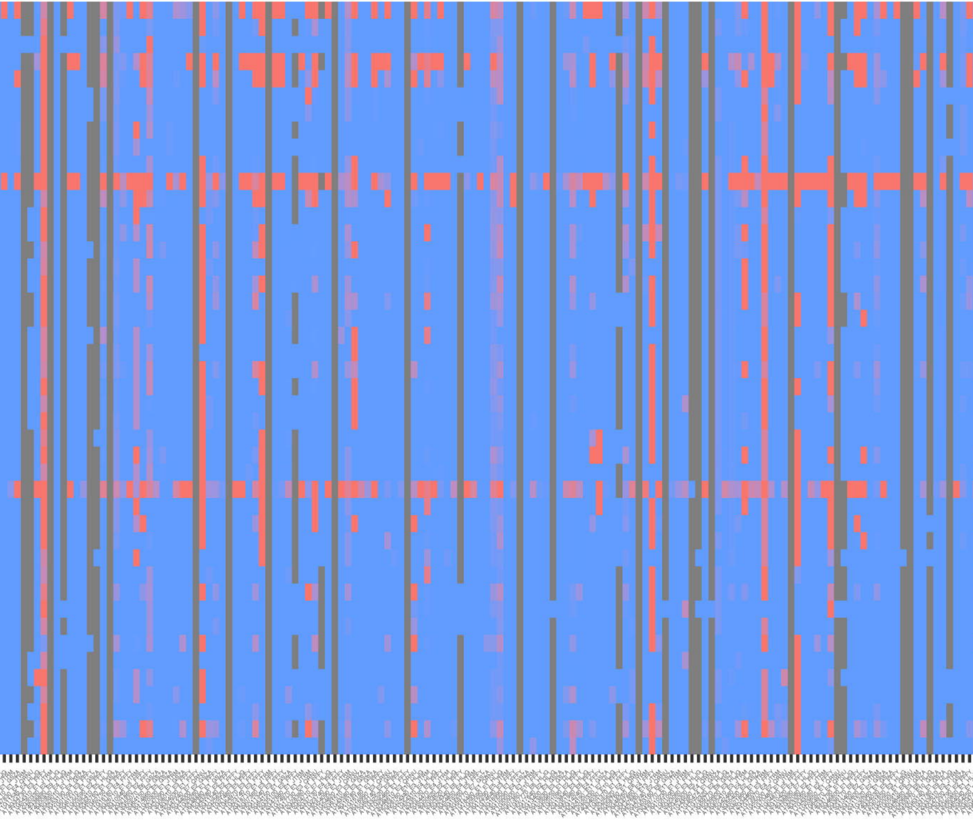

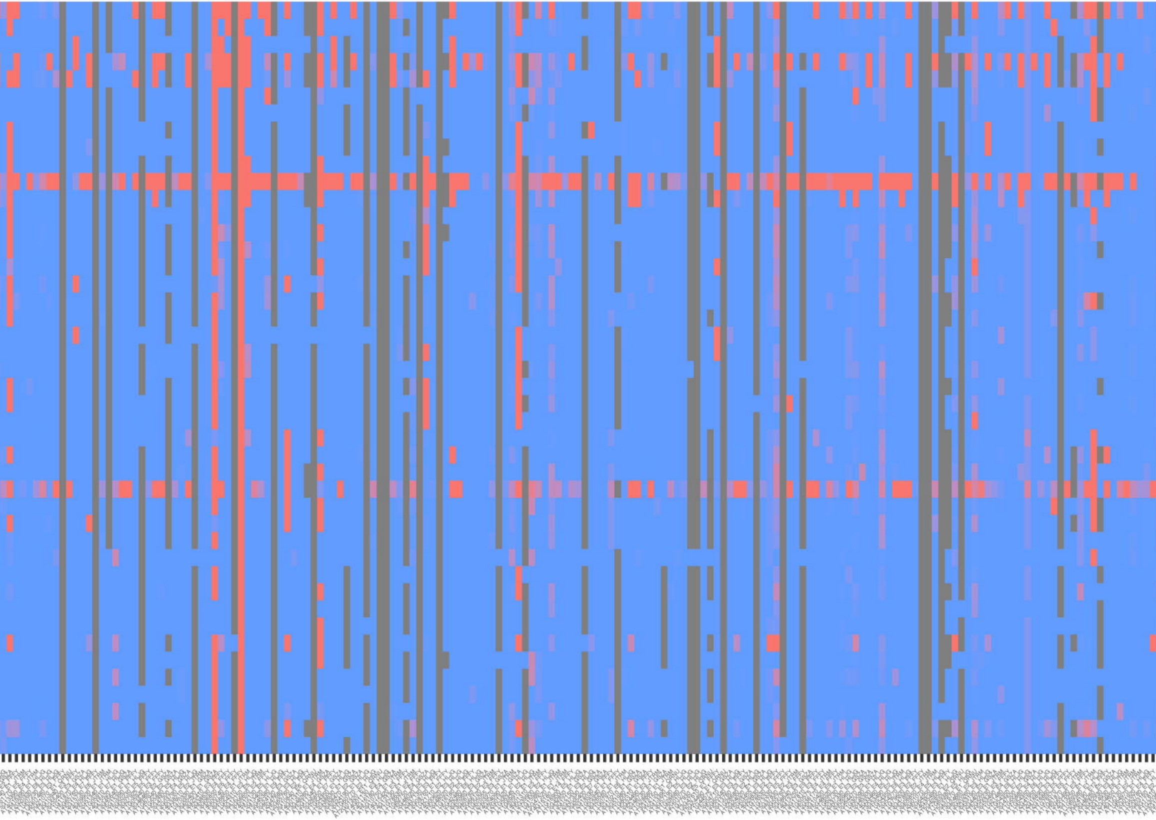

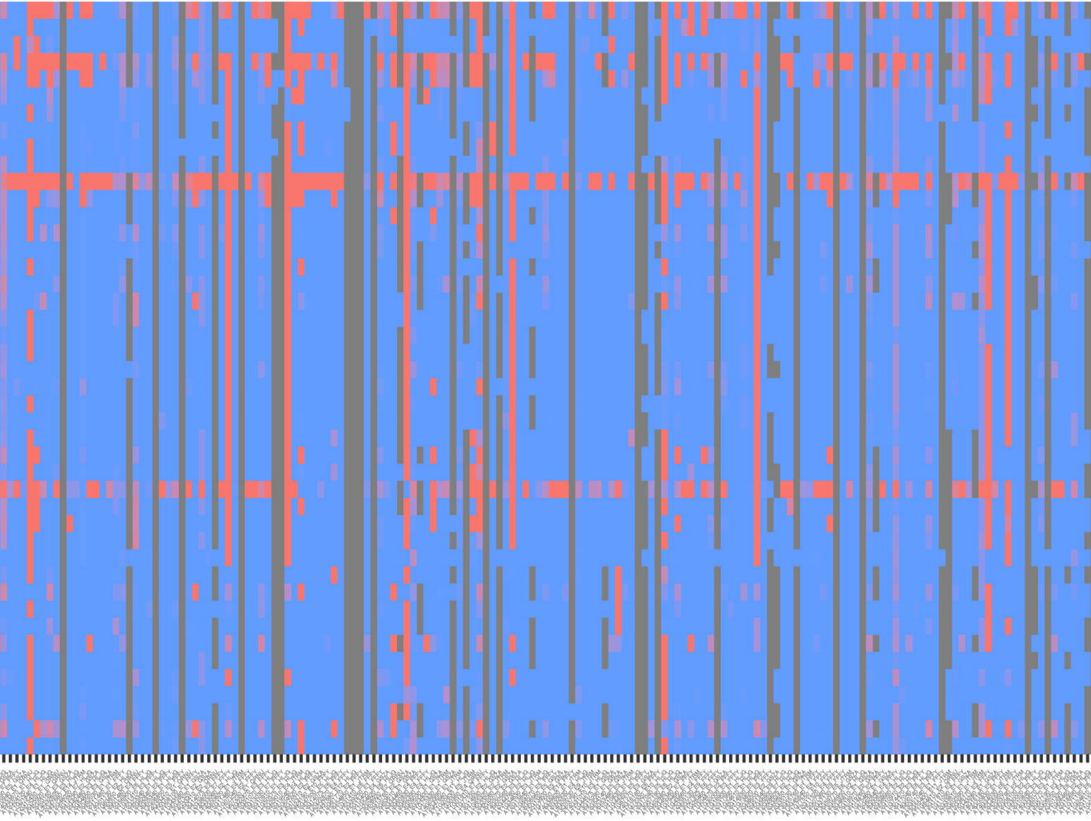

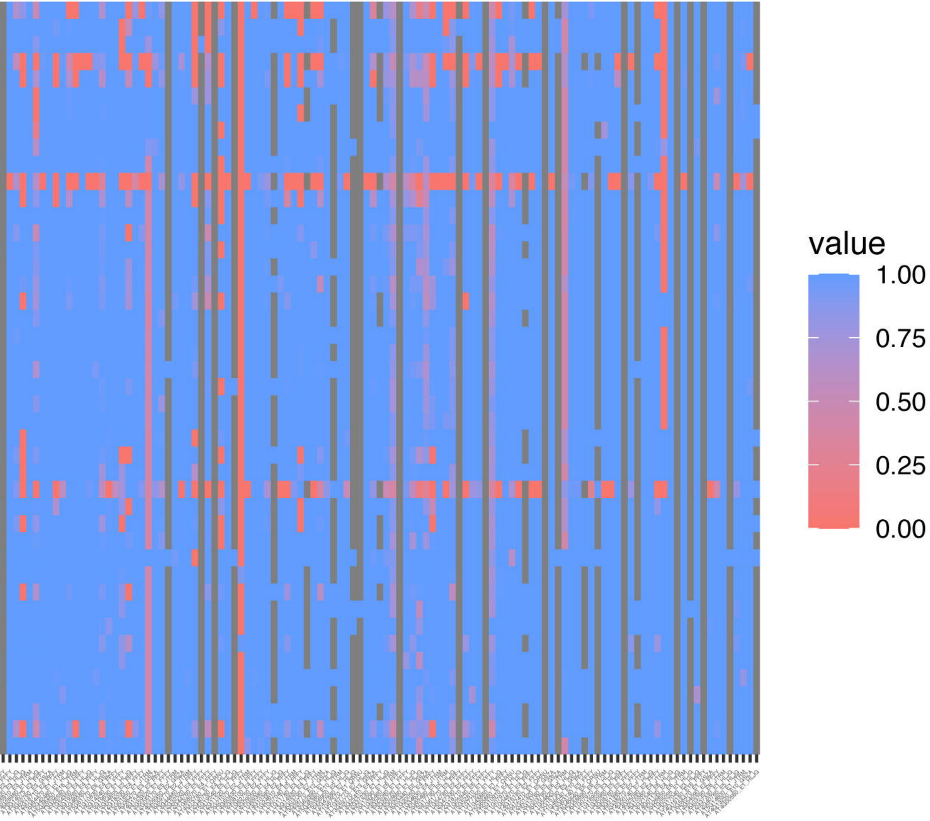
value
1.00
0.75
0.50
0.25
0.00

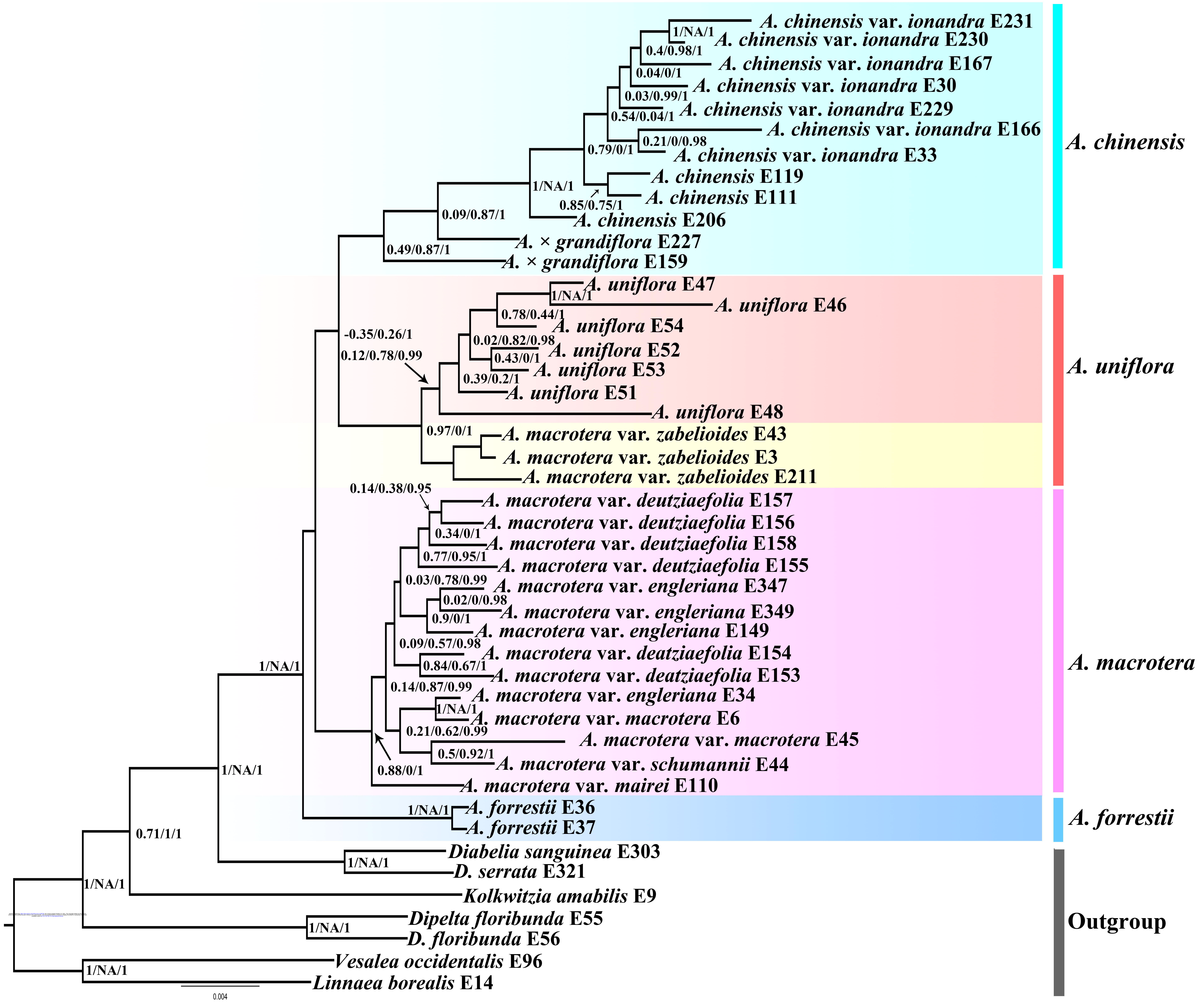
A. chinensis var. ionandra E231
1/NA/1
A. chinensis var. ionandra E230
0.4/0.98/1
A. chinensis var. ionandra E167
0.04/0/1
A. chinensis var. ionandra E30
0.03/0.99/1
A. chinensis var. ionandra E229
0.54/0.04/1
A. chinensis var. ionandra E166
0.21/0/0.98
0.79/0/1
A. chinensis var. ionandra E33
A. chinensis E119
1/NA/1
A. chinensis E111
0.85/0.75/1
A. chinensis E206
0.09/0.87/1
A. × grandiflora E227
0.49/0.87/1
A. × grandiflora E159
A. chinensis
A. uniflora E47
1/NA/1
A. uniflora E46
0.78/0.44/1
A. uniflora E54
-0.35/0.26/1
0.02/0.82/0.98
A. uniflora E52
0.12/0.78/0.99
0.43/0/1
A. uniflora E53
0.39/0.2/1
A. uniflora E51
A. uniflora E48
A. uniflora
0.97/0/1
A. macrotera var. zabelioides E43
A. macrotera var. zabelioides E3
A. macrotera var. zabelioides E211
0.14/0.38/0.95
A. macrotera var. deutziaefolia E157
A. macrotera var. deutziaefolia E156
0.34/0/1
A. macrotera var. deutziaefolia E158
0.77/0.95/1
A. macrotera var. deutziaefolia E155
0.03/0.78/0.99
A. macrotera var. engleriana E347
0.02/0/0.98
A. macrotera var. engleriana E349
0.9/0/1
A. macrotera var. engleriana E149
0.09/0.57/0.98
A. macrotera var. deatziaefolia E154
1/NA/1
0.84/0.67/1
A. macrotera var. deatziaefolia E153
A. macrotera
0.14/0.87/0.99
A. macrotera var. engleriana E34
1/NA/1
A. macrotera var. macrotera E6
0.21/0.62/0.99
A. macrotera var. macrotera E45
1/NA/1
0.5/0.92/1
A. macrotera var. schumannii E44
0.88/0/1
A. macrotera var. mairei E110
1/NA/1
A. forrestii E36
A. forrestii E37
A. forrestii
0.71/1/1
Diabelia sanguinea E303
1/NA/1
D. serrata E321
1/NA/1
Kolkwitzia amabilis E9
Dipelta floribunda E55
1/NA/1
D. floribunda E56
Outgroup
Vesalea occidentalis E96
1/NA/1
Linnaea borealis E14
0.004

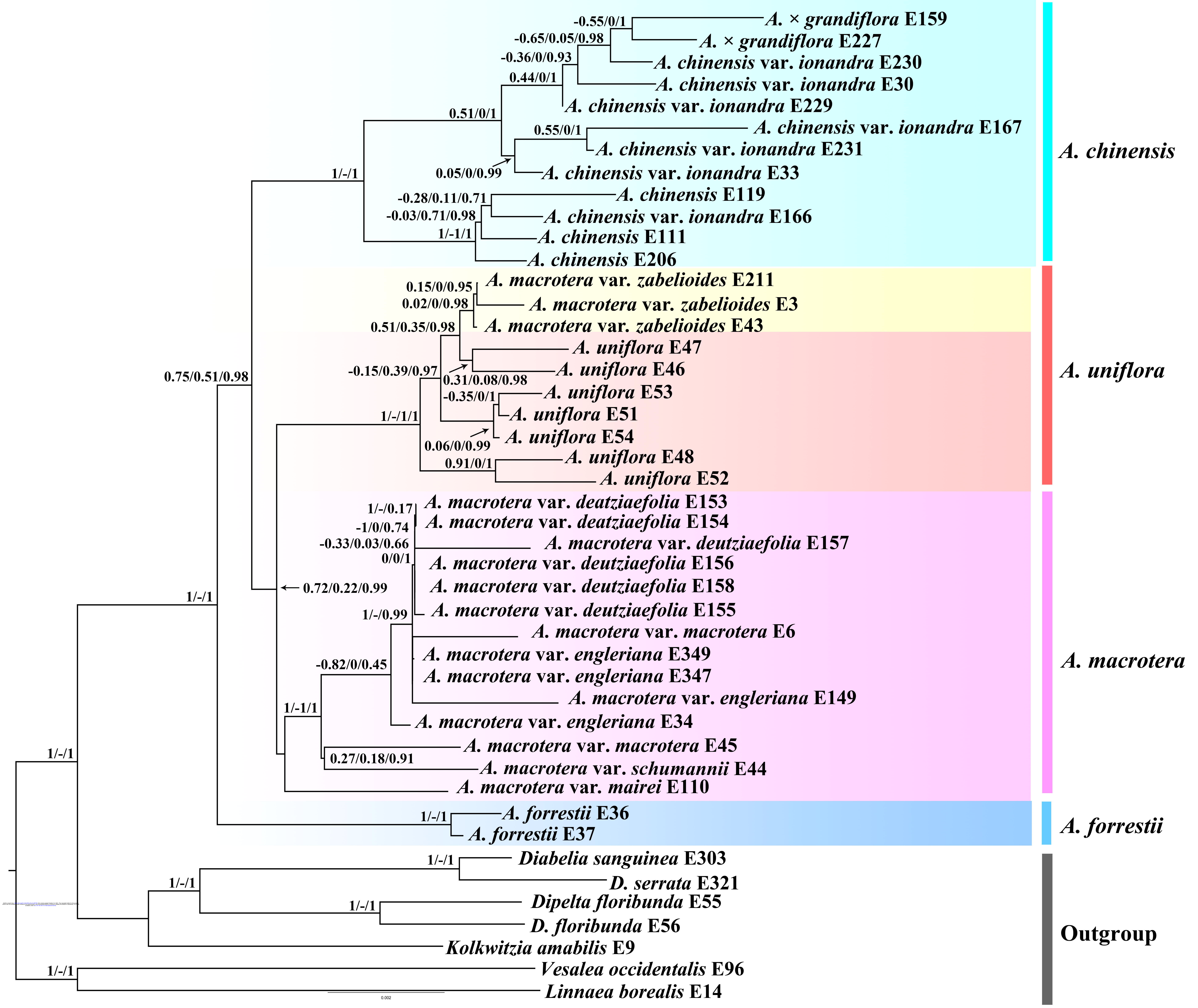
-0.55/0/1
A. × grandiflora E159
-0.65/0.05/0.98
A. × grandiflora E227
-0.36/0/0.93
A. chinensis var. ionandra E230
0.44/0/1
A. chinensis var. ionandra E30
A. chinensis var. ionandra E229
0.51/0/1
0.55/0/1
A. chinensis var. ionandra E167
A. chinensis var. ionandra E231
0.05/0/0.99
A. chinensis var. ionandra E33
1/-/1
-0.28/0.11/0.71
A. chinensis E119
-0.03/0.71/0.98
A. chinensis var. ionandra E166
1/-1/1
A. chinensis E111
A. chinensis E206
A. chinensis
0.15/0/0.95
A. macrotera var. zabelioides E211
0.02/0/0.98
A. macrotera var. zabelioides E3
0.51/0.35/0.98
A. macrotera var. zabelioides E43
A. uniflora E47
-0.15/0.39/0.97
A. uniflora E46
0.31/0.08/0.98
-0.35/0/1
A. uniflora E53
0.75/0.51/0.98
1/-/1/1
A. uniflora E51
A. uniflora E54
0.06/0/0.99
A. uniflora E48
0.91/0/1
A. uniflora E52
A. uniflora
A. macrotera var. deatziaefolia E153
1/-/0.17
A. macrotera var. deatziaefolia E154
-1/0/0.74
-0.33/0.03/0.66
A. macrotera var. deutziaefolia E157
0/0/1
A. macrotera var. deutziaefolia E156
0.72/0.22/0.99
A. macrotera var. deutziaefolia E158
1/-/1
A. macrotera var. deutziaefolia E155
1/-/0.99
A. macrotera var. macrotera E6
A. macrotera var. engleriana E349
-0.82/0/0.45
A. macrotera var. engleriana E347
A. macrotera var. engleriana E149
1/-1/1
A. macrotera var. engleriana E34
A. macrotera var. macrotera E45
1/-/1
0.27/0.18/0.91
A. macrotera var. schumannii E44
A. macrotera var. mairei E110
A. macrotera
1/-/1
A. forrestii E36
A. forrestii E37
A. forrestii
1/-/1
Diabelia sanguinea E303
1/-/1
D. serrata E321
1/-/1
Dipelta floribunda E55
D. floribunda E56
Kolkwitzia amabilis E9
Outgroup
1/-/1
Vesalea occidentalis E96
Linnaea borealis E14
0.002

A
A. forrestii E36
A. macrotera var. macrotera E45
A. macrotera var. schumannii E44
A. macrotera var. engleriana E149
A. macrotera var. deutziaefolia E157
A. macrotera var. deatziaefolia E154
A. uniflora E48
A. uniflora E46
A. macrotera var. zabelioides E43
0.589
A. × grandiflora E159
A. × grandiflora E227
0.411
A. chinensis E206
A. chinensis var. ionandra E33
A. chinensis E111
D. serrata E321
B
A. macrotera var. macrotera E45
A. macrotera var. schumannii E44
A. macrotera var. deatziaefolia E154
A. macrotera var. deutziaefolia E157
A. macrotera var. engleriana E149
A. × grandiflora E159
A. uniflora E46
A. macrotera var. zabelioides E43
A. uniflora E48
0.761
0.477
A. forrestii E36
A. chinensis E111
A. chinensis var. ionandra E33
A. chinensis E206
0.239
A. × grandiflora E227
0.523
D. serrata E321
C
A. forrestii E36
A. macrotera var. macrotera E45
A. macrotera var. schumannii E44
A. macrotera var. engleriana E149
A. macrotera var. deutziaefolia E157
A. macrotera var. deatziaefolia E154
A. uniflora E46
0.339
A. macrotera var. zabelioides E43
A. uniflora E48
0.812
0.406
A. × grandiflora E159
0.661
A. chinensis E206
0.188
0.594
A. × grandiflora E227
A. chinensis E111
A. chinensis var. ionandra E33
D. serrata E321
D
A. forrestii E36
A. macrotera var. macrotera E45
A. macrotera var. schumannii E44
A. macrotera var. deatziaefolia E154
A. macrotera var. deutziaefolia E157
A. macrotera var. engleriana E149
A. uniflora E48
0.428
A. macrotera var. zabelioides E43
A. uniflora E46
A. × grandiflora E159
0.536
0.572
0.259
A. × grandiflora E227
0.53
0.741
0.464
A. chinensis E206
0.47
A. chinensis E111
A. chinensis var. ionandra E33
D. serrata E321
E
A. chinensis var. ionandra E33
A. chinensis E111
0.468
0.155
A. × grandiflora E159
0.845
0.172
A. chinensis E206
0.828
0.482
A. × grandiflora E227
0.581
A. uniflora E46
A. uniflora E48
0.921
A. macrotera var. zabelioides E43
0.079
A. macrotera var. deutziaefolia E157
A. macrotera var. deatziaefolia E154
A. macrotera var. engleriana E149
A. macrotera var. schumannii E44
A. macrotera var. macrotera E45
A. forrestii E36
D. serrata E321

A
A. forrestii E36
0.317
A. macrotera var. macrotera E45
A. macrotera var. schumannii E44
A. macrotera var. engleriana E149
A. macrotera var. deatziaefolia E157
0.683
A. macrotera var. deutziaefolia E154
A. macrotera var. zabelioides E43
A. uniflora E46
A. uniflora E48
A. chinensis E111
A. chinensis var. ionandra E33
D. serrata E321
B
0.832
A. macrotera var. zabelioides E43
A. uniflora E46
A. uniflora E48
0.168
A. chinensis var. ionandra E33
0.5
A. chinensis E111
0.5
A. macrotera var. macrotera E45
A. macrotera var. deutziaefolia E154
A. macrotera var. deatziaefolia E157
A. macrotera var. engleriana E149
A. macrotera var. schumannii E44
A. forrestii E36
D. serrata E321
C
0.661
A. uniflora E48
A. uniflora E46
A. macrotera var. zabelioides E43
0.339
A. macrotera var. engleriana E149
A. macrotera var. deatziaefolia E15
0.762
A. macrotera var. deutziaefolia E15
A. macrotera var. schumannii E44
0.238
A. macrotera var. macrotera E45
A. forrestii E36
0.448
A. chinensis E111
0.552
A. chinensis var. ionandra E33
D. serrata E321
D
0.357
A. chinensis E111
0.796
0.634
A. chinensis var. ionandra E33
A. uniflora E48
0.707
0.293
0.835
A. macrotera var. zabelioides E43
A. uniflora E46
0.165
A. macrotera var. deatziaefolia E157
A. macrotera var. deutziaefolia E154
0.204
A. macrotera var. engleriana E149
A. macrotera var. macrotera E45
A. macrotera var. schumannii E44
A. forrestii E36
D. serrata E321
E
0.532
A. uniflora E48
0.468
A. macrotera var. zabelioides E43
A. uniflora E46
0.841
A. chinensis var. ionandra E33
A. chinensis E111
0.861
0.159
A. macrotera var. macrotera E45
0.738
A. macrotera var. schumannii E44
0.139
0.262
A. macrotera var. deatziaefolia E157
A. macrotera var. deutziaefolia E154
A. macrotera var. engleriana E149
A. forrestii E36
D. serrata E321

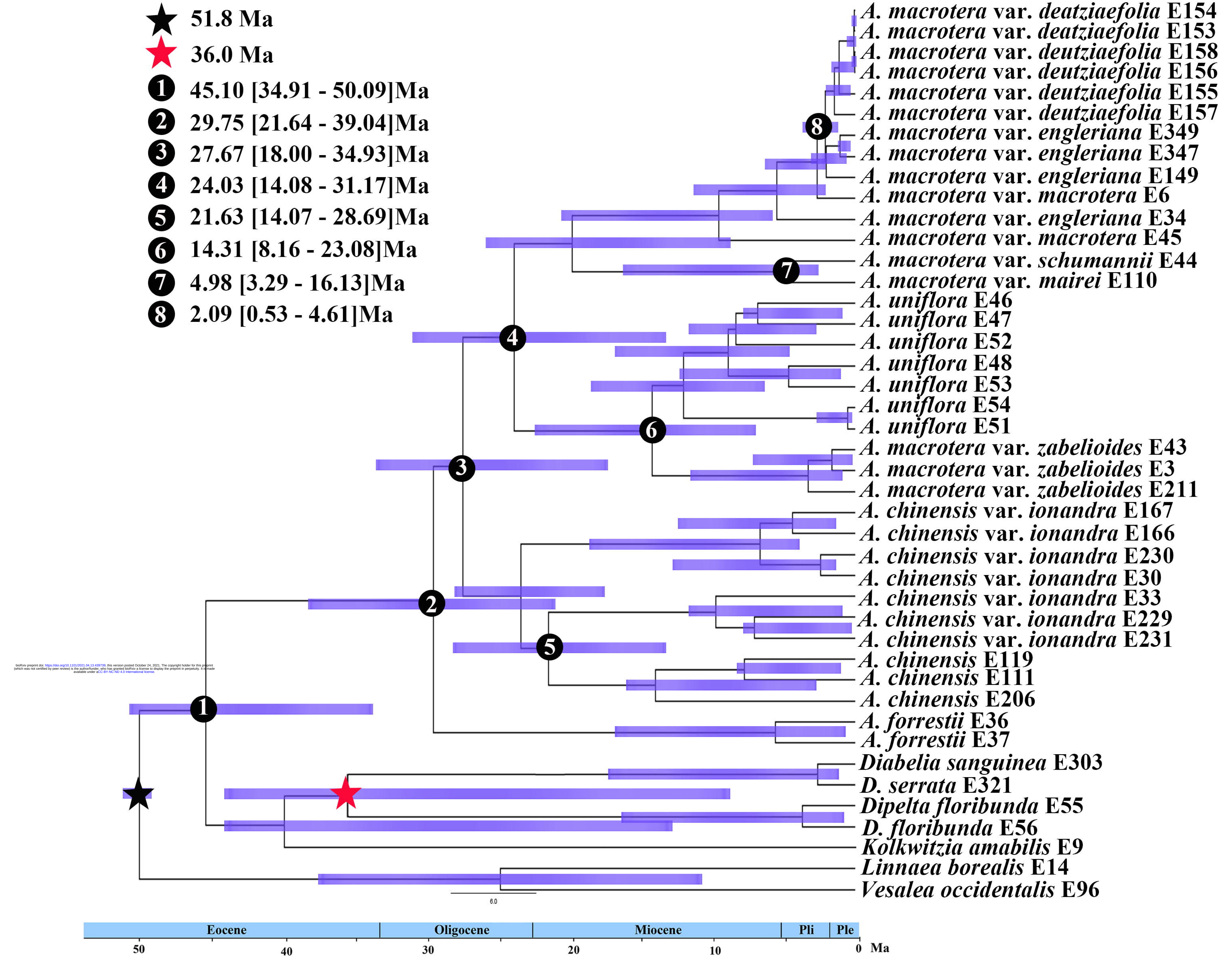
★ 51.8 Ma
★ 36.0 Ma
❶ 45.10 [34.91 - 50.09]Ma
❷ 29.75 [21.64 - 39.04]Ma
❸ 27.67 [18.00 - 34.93]Ma
❹ 24.03 [14.08 - 31.17]Ma
❺ 21.63 [14.07 - 28.69]Ma
❻ 14.31 [8.16 - 23.08]Ma
❼ 4.98 [3.29 - 16.13]Ma
❽ 2.09 [0.53 - 4.61]Ma
A. macrotera var. deatziaefolia E154
A. macrotera var. deatziaefolia E153
A. macrotera var. deutziaefolia E158
A. macrotera var. deutziaefolia E156
A. macrotera var. deutziaefolia E155
A. macrotera var. deutziaefolia E157
A. macrotera var. engleriana E349
A. macrotera var. engleriana E347
A. macrotera var. engleriana E149
A. macrotera var. macrotera E6
A. macrotera var. engleriana E34
A. macrotera var. macrotera E45
A. macrotera var. schumannii E44
A. macrotera var. mairei E110
A. uniflora E46
A. uniflora E47
A. uniflora E52
A. uniflora E48
A. uniflora E53
A. uniflora E54
A. uniflora E51
A. macrotera var. zabelioides E43
A. macrotera var. zabelioides E3
A. macrotera var. zabelioides E211
A. chinensis var. ionandra E167
A. chinensis var. ionandra E166
A. chinensis var. ionandra E230
A. chinensis var. ionandra E30
A. chinensis var. ionandra E33
A. chinensis var. ionandra E229
A. chinensis var. ionandra E231
A. chinensis E119
A. chinensis E111
A. chinensis E206
A. forrestii E36
A. forrestii E37
Diabelia sanguinea E303
D. serrata E321
Dipelta floribunda E55
D. floribunda E56
Kolkwitzia amabilis E9
Linnaea borealis E14
Vesalea occidentalis E96
1
2
3
4
5
6
7
8
6.0
Eocene
Oligocene
Miocene
Pli
Ple
50
40
30
20
10
0
Ma

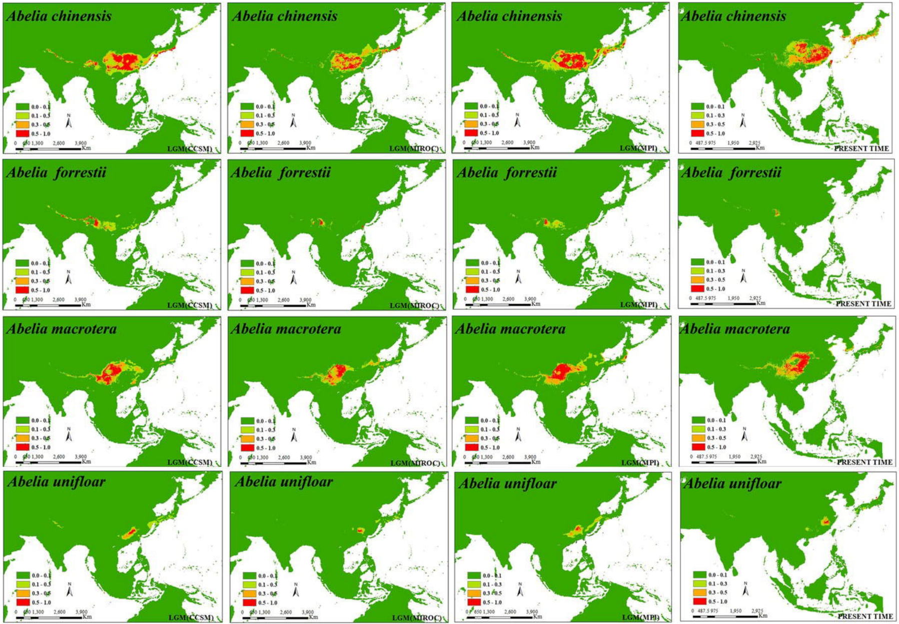
Abelia chinensis
0.0 - 0.1
0.1 - 0.3
0.3 - 0.5
0.5 - 1.0
N
0 650 1,300 2,600 3,900 Km
LGM(CCSM)
Abelia chinensis
LGM(MIROC)
Abelia chinensis
LGM(MPI)
Abelia chinensis
0 487.5 975 1,950 2,925 Km
PRESENT TIME
Abelia forrestii
LGM(CCSM)
Abelia forrestii
LGM(MIROC)
Abelia forrestii
LGM(MPI)
Abelia forrestii
PRESENT TIME
Abelia macrotera
LGM(CCSM)
Abelia macrotera
LGM(MIROC)
Abelia macrotera
LGM(MPI)
Abelia macrotera
PRESENT TIME
Abelia unifloar
LGM(CCSM)
Abelia unifloar
LGM(MIROC)
Abelia unifloar
LGM(MPI)
Abelia unifloar
PRESENT TIME

Table. S1 The 19 bioclimatic variables for ENM analyses

Code	**Variable**
BIO1	Annual Mean Temperature
BIO2	Mean Diurnal Range [Mean of monthly (max temp-min temp)]
BIO3	Isothermality (BIO2/BIO7) (* 100)
BIO4	Temperature Seasonality (standard deviation *100)
BIO5	Max Temperature of Warmest Month
BIO6	Min Temperature of Coldest Month
BIO7	Temperature Annual Range (BIO5-BIO6)
BIO8	Mean Temperature of Wettest Quarter
BIO9	Mean Temperature of Driest Quarter
BIO10	Mean Temperature of Warmest Quarter
BIO11	Mean Temperature of Coldest Quarter
BIO12	Annual Precipitation
BIO13	Precipitation of Wettest Month
BIO14	Precipitation of Driest Month
BIO15	Precipitation Seasonality (Coefficient of Variation)
BIO16	Precipitation of Wettest Quarter
BIO17	Precipitation of Driest Quarter
BIO18	Precipitation of Warmest Quarter
BIO19	Precipitation of Coldest Quarter

Table S2. HybPiper assembly statistics

Species	Number of reads	Number of reads on target	Percent reads on target	Number of exons with reads	Number of exons with contigs	Number of exons with sequences	Number of exons with sequences > 25% of the target length	Number of exons with sequences > 50% of the target length	Number of exons with sequences > 75% of the target length	Number of exons with sequences > 150% of the target length	Number of exons with paralog warnings
A. chinensis E111	12086904	4547698	0.376	1094	1010	985	983	966	907	0	123
A. chinensis E119	14252558	4342227	0.305	1098	999	972	970	957	906	1	93
A. chinensis E206	9076240	3538761	0.39	1118	1021	994	993	979	930	1	162
A. chinensis var. *ionandra* E30	8512137	2058453	0.242	1054	969	945	942	917	835	1	72
A. chinensis var. *ionandra* E33	15488895	4871294	0.315	1094	999	973	971	960	915	2	86
A. chinensis var. *ionandra* E166	3560876	749920	0.211	1057	966	948	941	893	763	1	60
A. chinensis var. *ionandra* E167	4799543	1123534	0.234	1103	982	962	960	930	863	1	96
A. chinensis var. *ionandra* E229	8420983	2523313	0.3	1110	1014	985	983	963	914	1	90
A. chinensis var. *ionandra* E230	11800314	4525033	0.383	1121	1012	983	982	967	927	2	93
A. chinensis var. *ionandra* E231	9802195	1723306	0.176	1155	1036	1012	1011	994	941	3	140
A. forrestii E36	32830208	9311224	0.284	1160	1051	1011	1010	994	954	1	159
A. forrestii E37	9666409	2890168	0.299	1114	1005	977	975	961	921	0	78
A.× grandiflora E159	9807596	3364549	0.343	1121	1027	997	995	975	930	1	219
A.× grandiflora E227	12254174	4742077	0.387	1133	1039	1010	1010	993	944	1	271
A. macrotera var. *mairei* E110	9134947	2888390	0.316	1072	988	960	959	940	901	1	94
A. macrotera var. *deutziaefolia* E153	7647999	2528861	0.331	1125	1016	985	982	954	893	0	95
A. macrotera var. *deutziaefolia* E154	10129358	3237016	0.32	1130	1016	979	978	963	921	0	100
A. macrotera var. *deutziaefolia* E155	4426579	1033080	0.233	1103	987	966	962	933	860	0	70
A. macrotera var. *deutziaefolia* E156	9536952	3305495	0.347	1130	1017	978	977	959	918	0	102

A. macrotera var. *deutziaefolia* E157	4754995	1345791	0.283	1096	988	959	958	943	892	1	89
A. macrotera var. *deutziaefolia* E158	9445133	2856721	0.302	1113	1009	971	969	953	915	0	100
A. macrotera var. *engleriana* E34	7200184	1795642	0.249	1099	1003	971	970	953	905	1	83
A. macrotera var. *engleriana* E149	11394102	3988828	0.35	1114	1020	986	984	968	920	0	99
A. macrotera var. *engleriana* E347	8183348	1385872	0.169	1103	990	960	958	941	893	0	82
A. macrotera var. *engleriana* E349	6925508	1478921	0.214	1105	993	966	966	943	863	0	73
A. macrotera var. zabelioides E3	5493922	1344879	0.245	1076	987	963	963	946	904	1	88
A. macrotera var. zabelioides E43	6885612	1741233	0.253	1085	1000	971	971	956	914	1	87
A. macrotera var. zabelioides E211	4278814	878749	0.205	1068	978	949	946	921	846	0	68
A. macrotera var. *macrotera* E6	5223871	1429204	0.274	1063	990	959	958	938	874	0	83
A. macrotera var. *macrotera* E45	1833543	32422	0.018	825	436	424	417	355	253	0	6
A. uniflora E46	16490536	3625219	0.22	1133	1064	1042	1042	1028	992	0	698
A. uniflora E47	3257944	439031	0.135	1068	945	924	924	904	858	1	120
A. uniflora E48	1922338	260996	0.136	958	734	715	696	587	423	0	19
A. uniflora E51	18769946	3613529	0.193	1086	991	967	966	946	892	2	103
A. uniflora E52	2713371	576730	0.213	1039	954	930	929	913	871	1	80
A. uniflora E53	2724962	439041	0.161	1038	943	921	920	902	855	0	75
A. uniflora E54	15998204	2846753	0.178	1079	992	968	967	943	900	1	103
A. schumannii E44	2391304	253742	0.106	1038	897	877	874	847	775	0	67
Diabelia sanguinea E303	10970170	3075238	0.28	1134	1025	991	988	973	914	0	91
D. serrata E321	13220295	4190116	0.317	1138	1037	1002	1000	986	934	0	93
Dipelta floribunda E55	4636783	105360	0.023	924	660	642	639	601	507	0	27
D. floribunda E56	6580640	248258	0.038	992	853	833	830	793	680	0	43
Kolkwitzia amabilis E9	9779050	2641147	0.27	1097	1005	984	983	967	916	0	75
Linnaea borealis E14	9523146	1355451	0.142	1069	981	962	961	946	902	1	73

Vesalea occidentalis E96	6434742	142056	0.022	974	730	712	703	650	559	0	23